

Tesis defendida por
Jhonnatan Guerrero Muñoz

y aprobada por el siguiente Comité

Dr. Víctor Ruiz Cortés
Codirector del Comité

Dr. Cyrille Vezy
Codirector del Comité

Dr. Heriberto Márquez Becerra
Miembro del Comité

Dr. Jorge Olmos Soto
Miembro del Comité

Dr. Josué Álvarez Borrego
Miembro del Comité

Dr. Pedro Negrete Regagnon
Coordinador
Posgrado en Óptica

Dr. Jesús Favela Vara
Director
Dirección de Estudios de Posgrado

Mayo de 2014

CENTRO DE INVESTIGACIÓN CIENTÍFICA Y DE EDUCACIÓN
SUPERIOR DE ENSENADA, BAJA CALIFORNIA



Programa de posgrado en ciencias
en Óptica

Microfluidic device for the study of adhesion in living cells by microscopy

Tesis

para cubrir parcialmente los requisitos necesarios para obtener el grado de

Maestro en Ciencias

Presenta:

Jhonnatan Guerrero Muñoz

Ensenada, Baja California, México,

2014

Resumen de la tesis de Jhonnatan Guerrero Muñoz, presentada como requisito parcial para la obtención del grado de Maestro en Ciencias en Óptica con orientación en Optoelectrónica.

Dispositivo microfluídico para el estudio de adhesión de células vivas por microscopía

Resumen aprobado por:

Dr. Víctor Ruiz Cortés

Codirector de Tesis

Dr. Cyrille Vezy

Codirector de Tesis

Esta tesis muestra un estudio teórico y experimental de diferentes áreas como la microfluídica, la óptica y la biología para acoplar en un solo dispositivo para una aplicación biofotónica. Un generador de gradientes de 2 entradas se realiza mediante fotolitografía utilizando una deposición de fotoresina SU-8 2050 por centrifugado para el dispositivo maestro. El dispositivo de microfluidos se realizó con polidimetilsiloxano (PDMS) y se unió a un cubreobjetos de vidrio por grabado por reacción de iones (RIE). El dispositivo de microfluidos fue adaptado para formar parte de un sistema de microscopía de contraste de interferencia por reflexión (RICM). Los resultados muestran que el paso de revelado es un paso crítico para asegurar buenos dispositivos microfluídicos.

El generador de gradientes se caracteriza por intensidad. Primero, fluyendo una sustancia de color (permanganato de potasio) en una entrada y de agua en el otro a una velocidad de 0.4ml/minute. La toma de imágenes fue realizada con un microscopio convencional. Después se realizó otro experimento en el cual se hizo fluir partículas fluorescentes (Alexa488) en una entrada y agua en la otra. La toma de imágenes fue realizada en un sistema de microscopía de fluorescencia, obteniendo en ambos casos un gradiente bien definido.

Un sistema de RICM fue construido principalmente usando un microscopio Zeiss, un fotodiodo como una fuente con una longitud de onda de $\lambda = 658\text{nm}$ y un difusor. Esta técnica se utilizó para medir el radio de curvatura de partículas esféricas de una manera muy precisa y después se utilizó esta información para encontrar la distancia de la partícula a la superficie, se obtuvo una distancia de separación de $0,389\ \mu\text{m}$ para partículas esféricas de $R = 10.018\ \mu\text{m}$.

También se hizo el cultivo de células MDA MB 231 mediante el proceso convencional para cultivo celular y tratamos de fijar las células en un entorno microfluídico encontrando problemas de burbujas y de presión cuando fluye medio de cultivo fresco.

Palabras Clave: **RICM, Microfluídica, Microscopía, Biofotónica**

Abstract of the thesis presented by Jhonnatan Guerrero Muñoz, in partial fulfillment of the requirements of the degree of Master in Sciences in Optics with orientation in Optoelectronics.

Microfluidic device for the study of adhesion in living cells by microscopy

Abstract approved by:

Dr. Víctor Ruiz Cortés

Codirector de Tesis

Dr. Cyrille Vezy

Codirector de Tesis

This thesis shows the study theoretical and experimental of different areas such as microfluidics, optics and biology in order to couple them into a single device for biophotonics application. A gradient generator of 2 inlets is made by photolithography using a deposition of SU-8 2050 photoresist by spincoat for the master device. The microfluidic device was made with Polydimethylsiloxane (PDMS) and was bonded to a glass coverslip by Reactive-Ion Etching (RIE). The microfluidic device was adapted to form part of a reflection interference contrast microscopy system (RICM). The results shows that developing is a critical step to ensure good microfluidic devices.

The gradient generator was characterized by intensity. First, flowing a colored substance (potassium permanganate) in one inlet and water in the other at 0.4ml/minute and taking pictures on a conventional microscope. After flowing fluorescent probes (Alexa488) and water and taking pictures at a fluorescent microscope system obtaining in both cases a very well defined gradient.

A RICM system was build mainly using a ZEISS microscope, a photodiode as a source with a wavelength of $\lambda = 658\text{nm}$ and a diffuser. This technique was used to measure the radius of curvature of spherical beads very accurately and after, using this information to find the distance from the particle to the surface obtaining a separation distance of $0.389\mu\text{m}$ for spherical beads of $R = 10.018\mu\text{m}$.

We also did cell culture of MDA MB 231 under conventional process for cell culture and tried to set the cells under microfluidic environment getting some bubbles and pressure problems when flowing fresh medium.

Keywords: **RICM, Microfluidics, Microscopy, Biophotonics**

To my parents. Who gave me their unconditional support and motivated me to carry on proudly, no matter how difficult was the way.

Acknowledgements

To my family who always give me their empathy and cheer me up in every step I take in my life always thrusting that i will take wise decisions.

To my friends, the old ones and the new ones. Friends that had always been there sharing good and bad moments.

To my professors and classmates from the optics department who shared their study time and living lessons with me. To the CPP who thrust me in this international project and also to CICESE for being my second home. To Dr. Heriberto Márquez and Dr. Rafael Salas, who willed to help me to make this project became reality by linking me. Special thanks to Dr. Heriberto Marquez for his aid in professional and personal situations when I mostly needed. Also special thanks to Dr. Cyrille Vezy for helping me in everything he could, for tutoring me and also being very friendly with me, for accepting me in this project and having patience to guide me.

To Dr. Victor Ruíz for his friendship and support all this time, for helping and advising me in this important project for me. To Dr Jorge Olmos, Dr Josué Álvarez for being part of this project.

To l'Université de Technologie de Troyes and LNIO for their hospitality and disposition also to the city of Troyes for making my internship a pleasure. To Congreso Nacional de Ciencia y Tecnología (CONACyT) project No 51144-Y for its economical aid.

Finally i want to thanks everyone that was involved directly or indirectly with my life during the development of this project.

Table of contents

Resumen en español	II
Abstract in english	III
Dedicatory	IV
Acknowledgements	V
List of figures	XI
List of tables	XII
1. Introduction	1
2. State of art	5
2.1 Cell Mechanics	5
2.1.1 Cell adhesion and cell migration	5
2.2 Directed cell migration	7
2.3 Microfluidics	8
2.3.1 Laminar flow	9
2.3.2 Slow diffusion	11
2.4 Microfluidics for biology	12
3. Fabrication of microfluidic devices	13
3.1 Soft Lithography	14
3.1.1 Cleaning of the substrate	14

3.1.2	Deposition by spin coat	15
3.1.3	Pre-exposure bake	16
3.1.4	Exposition	16
3.1.5	Post-exposure bake	16
3.1.6	Developing process	17
3.2	Casting process with Polydimethylsiloxane (PDMS)	20
3.2.1	Punching Inlets	23
3.3	PDMS bonding by means of Reactive-Ion Etching (RIE)	23
3.4	Tubing and pressure control	25
3.5	Optimizing the process	26
3.5.1	Dilution	26
3.5.2	Double Layer	27
3.5.3	Optimal Parameters	28
4.	Experimental methods	29
4.1	Microscopy	29
4.1.1	Reflection Interference Contrast Microscopy (RICM)	30
4.1.2	Characterization of the RICM	35
4.1.3	MDA MB 231 cell observation	38
4.2	Gradient generator	41
4.2.1	Mathematical description	42
4.2.2	The mixing chamber	46
4.2.3	The step profile	47
4.2.4	The linear profile	50
5.	Cell fixing in microfluidics	52

5.1	Maintaining cultured cells	52
5.2	Cell fixing in a microfluidic device	53
6.	Conclusion and perspectives	56
	Bibliographic references	58

List of figures

1	Schematic representation of a the microfluidic gradient generator.	3
2	Schematic representation of a cell displacing, where the red spots corresponds to the adhesion points in the surface.	7
3	Structure of an adhesion complex in a migrating cells.	8
4	General steps of the photolithography process. A: Photoresist deposit by spin coating. B: Exposition to UV light. C: Development of the device in SU-8 developer. D: Cleaning of the unexposed photoresist with isopropanol.	13
5	Photography of the ultra sonic bath process to clean the substrate.	15
6	Photography of the spin coater at the clean room.	15
7	Photo of a device ready to be exposed in the photo masker	16
8	Photography of the hot plates with two devices under the hard bake step.	17
9	Master device after development. It can be seen some photoresist in the edges in the edges of the substrate.	22
10	methyl group transformed into silanol group.	24
11	Silanol group transformed into siloxane group.	25
12	Photography of the microfluidic system tubed.	26
13	Correspondence between photoresist layer thickness and the rotational speed of the spin coater for a 20 percent diluted SU-8 2050 in cyclohexanone.	27

14	RICM principle: A monochromatic light of intensity I_0 and wave length λ is sent to a cell adjacent to a surface. There formation of interference between the beams reflected by the surface of intensity I_1 , and those reflected by the cell of intensity I_2 . n_1 is the refractive index of the medium. The measurement of the interferogram provides the distance $h(x)$ between the cell and the coverslip.	31
15	Representation of a spherical bead of radius R separated a distance h from the surface.	32
16	Picture of the system components at LNIO. A is the photodiode, B is the aspherical lens covered in black paper, C is the diffuser covered in black paper, D is a converging lens, E is the diaphragm, F is the mirror and G is a converging lens.	32
17	Schematic diagram of the ilumination system for the RICM. Letters A to G are relating to figure 16 components.	33
18	Schematic diagram of the microscope components, showing 2 crossed polarisers, dichroic mirror, CCD camera and a objective with a build in quarter-wave plate. . .	33
19	Interference pattern of a spherical bead.	36
20	Correspondence between the position and the width in the horizontal axis.	36
21	Correspondence between the position and the width in the vertical axis.	37
22	Image of an spherical bead interference pattern and the calculated center pixel. . .	37
23	Correspondence between the position and the intensity.	38
24	Correspondence between the position of the maximums and the distance from the surface.	39
25	A: Picture of the cell in phase contrast.B: Picture of the cell in RICM.	39
26	A: Picture of the cell in phase contrast. B: Picture of the cell in RICM.	40
27	Optical microscopy image showing a microchanel with a U shape of the gradient generator device.	41

28	Optical microscopy image showing a microchanel of a five channel joint of the gradient generator device.	42
29	Christmas tree microfluidic network geometry.	43
30	Equivalent electric circuit model of a single branch.	43
31	Schematic representation for the nomenclature we used for the mathematical description of the network. If B=6 and S=2, for this branching point $R_1= 2R$ and $R_2= 5R$	45
32	Image of the outlet channel showing the gradient line profile for two different positions along the outlet channel under a flow rate of 0.4 ml/minute. a: 200 μm from the joint. b: 2000 μm from the joint.	47
33	Correspondence between intensity and position at 200 μm from the joint for the dye solution experiment.	48
34	Correspondence between intensity and position at 2000 μm from the joint for the solution experiment.	49
35	Gradient line profile at 5000 μm from the joint at the outlet channel under a flow rate of 0.4 ml/minute.	49
36	Correspondence between intensity and position at 5000 μm from the joint for the fluorescent particles solution experiment.	50
37	Gradient line profile at 5000 μm from the joint at the outlet channel under a flow rate of 0.01 ml/minute.	51
38	Correspondence between intensity and position at 5000 μm from the joint for the dye solution experiment.	51
39	Living MDA MB 231 cells attached in the substrate in a microfluidic device.	55

List of tables

1	Parameters used in the baking process.	17
2	Tests done for manual development, showing no real success in being a reliable process.	18
3	Tests done for vortex development, shown to be a reliable process but not as accurate as needed.	19
4	Tests done for ultrasonic development, showing an optimum development time of 45 seconds.	20
5	Tests done for exposition time, showing a 12 seconds exposition time under a UV lamp power of 8.5 mJ/cm ² s.	21
6	Tests done for RIE process. Optimal parameters are highlighted.	25

Chapter 1

Introduction

One of the biggest challenges in biomedicine is the study of cancer cells, with two mayor problems to overcome. The first one, a system to emulate the environment in which the cells are immerse. The second, to have a compatible system to quantify the phenomena. With these conditions there is a need to implement a technique that is capable of generating and maintaining adequate stable conditions for long periods of time. To solve the first problem microfluidics is a good option.

It is well known that a cancer tumour can cause invasive phenotypes which travel through the bloodstream and lymphatic circulatory system to eventually settle down into a new body and proliferate, this process is known as metastasis. Some research (Wang *et al.*, 2004]) has proved that in metastasis of cancer cells are directed to their targets by soluble factors secreted by the organs to be invaded, this would imply that the migration of cancer cells is directed, being the investigation of chemotaxis (movement induced by changes in the concentration) crucial for understanding metastasis (De Robertis, 1968).

Commonly used equipment such as chemotaxic chambers or introducing pipetted flows have two major problems, one of them is the low diversity of chemical gradients that can be generated and the second is the difficulty in maintaining stable generated gradient by long periods of time. Microfluidic devices are an alternative to these methods to meet those needs (Dertinger *et al.*, 2000).

The use of microfluidic devices for biomedical research and develop technologies for clinical use have several advantages. First, the volume of fluid in the channel is very

small, usually a few nanolitres whereby the number of substrates and reagents used is very small. This is especially significant when working with expensive reagents. Second, the manufacturing techniques used to construct microfluidic devices are relatively inexpensive and currently exist techniques for the mass reproduction of them. There is great interest in investigating the role of chemical gradients in biological systems, such research would benefit greatly by having a technique for producing gradients with complex profiles (Stephan *et al.*, 2001).

The total internal reflection microscopy is a non-invasive technique for obtaining information about the position of objects near the surface (Laurent, 2009), this technique provides a high spatial resolution. Since the field of application of this technique are small scale (of the order of nanometres), makes it a technique in which large samples are not required.

Current methods to study cell response in presence of biochemical signals are expensive and limited in the number of tests that can be performed simultaneously (Whitesides *et al.*, 2001). Developing a technology that could analyse the behaviour of cell response to chemical gradients could lead to advancements in different fields like tissue engineering, drug discovery and biomedicine.

To overcome the difficulties associated with generating chemical gradient, a microfluidic system prototype was design and fabricated with polydimethylsiloxane(PDMS), the scheme of the microfluidic is shown in figure 1. In this research and previous studies (Dertinger *et al.*, 2001) have shown that the gradient generator is able to generate stable concentration gradients through a series of mixing and redistribution of the chemical reagents in the serpentine channels.

The microfluidic device system could be used to perform tests on cell behaviour with different gradient factors. Studies have proven that breast cancer cells (MDA

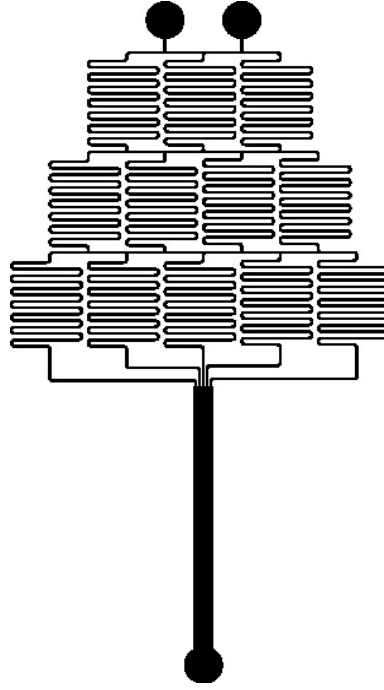


Figure 1. Schematic representation of a the microfluidic gradient generator.

MB 231 cell line) response to epidermal grow factor gradients (Wang *et al.*, 2004). Thus, the fabricated microfluidic gradient generator system has potential for many applications relating to various biomedical research. This research demonstrate that the system provides a way to conduct study and analysis on cell response to chemical gradients. In order to study cell adhesion and cell migration studies have been shown that reflection interference contrast microscopy (RICM) could be used to do single cell observation (Laurent, 2009). Cells dynamics like spreading (Sengupta, 2006) and membrane fluctuations (Zidovska, 2011) had been studied with RICM previously.

In this thesis the design and fabrication of a microfluidic system for total internal reflection microscopy is presented. In addition several fields are involved, such as biological phenomena, microfluidic devices and microscopy techniques with the aims to describe and to understand the basic processes for creating microfluidic devices by

photolithography, recognize the main parameters for the creation of the device and to propose a way to optimize the process.

The microchanelles were made using PDMS on a SU-8 2050 photoresist master device made by a photolithography process.

Chapter 2 is dedicated to state of the art where the basic principles involved are explained. Chapter 3 contains information about the manufacturing process of the microfluidic device. Chapter 4 is dedicated to the presentation of the system used in this work which includes system characterization and measurements made with it. Chapter 5 contains the cell culture protocol and insertion in the microfluidic environment. Chapter 6 contains the conclusion and perspectives for further work.

Chapter 2

State of art

In biology, every single process have several complexities and needs. One of those needs is a system to emulate the environment and, at the same time, allowing us to interact with the living process, therefore, it is necessary the implementation of a device that would satisfy these conditions. For this reason, in biomedicine as in many other areas of science, exist the need for interdisciplinary work, unifying different areas of knowledge like physics, biology, engineering among others.

2.1. Cell Mechanics

It is well known (De Robertis, 1968) that when a cancer tumour is generated in an afflicted zone it can produce invasive phenotypes of cells which can travel along the blood torrent through the sanguine system to finally invade and proliferate in a new organ giving rise to a new tumour, therefore, making it hard to control this disease. This kind of invasive process is known as metastasis. To understand the general concept of metastasis is required to study the cellular adhesion and cellular migration.

2.1.1. Cell adhesion and cell migration

Cell migration process is complex and not very well understood and it is involved in many physiologic as well pathologic phenomena (De Robertis, 1968). It can be seen in the early steps of embryogenesis when the cells migrate to the embryo, in the wound healing process when cells are released before and during the proliferative phase in order to reproduce and replace the dead cells, in the inflammatory response and many other

processes.

It also occurs in pathologic phenomena like metastasis as well as angiogenesis which is coupled to the wound healing response and tumour blood vessels.

There are many forms of celular motility like ciclosis, which is the internal movements of the cell without modifying the membrane, ameboidism which consist in the displacement due to the emission of pseudopods, ciliar and flagelar in which both are related to common mechanical displacement provided by the motion of cilios and flagelos respectively.

Due to the nature of the cells of interest, ameboidism movement is a topic in cell migration research (De Robertis, 1968). This movement is originated by the extension of pseudopods through which the cytoplasm flows, during the movement, the cell is constantly changing its shape as shown in figure 2.

This type of movement requires the adhesion to a solid support in order to exert the proper force that would lead to a displacement. The parts of the cell which plays a role are the cytoskeleton, adhesion molecules and extra celular matrix as shown in figure 3.

The cytoskeleton is made of microtubules and filaments, this constitute an elastic support that allows the cell to stretch and contract to modify its shape.

The adhesion molecules are a group of proteins localized in the surface of the celular membrane, the function of them is give stability to the cell by making contact with a surface or with another cell. Within this molecules exists some macromolecules named focal points who are in charge of sending signals to make the cell produce a directed mechanical forces in order to produce displacement of the membrane (De Robertis, 1968).

The focal points are bonded to the extra celular matrix, providing enough information to move along it, once they are bonded, the cell use them as stationary support

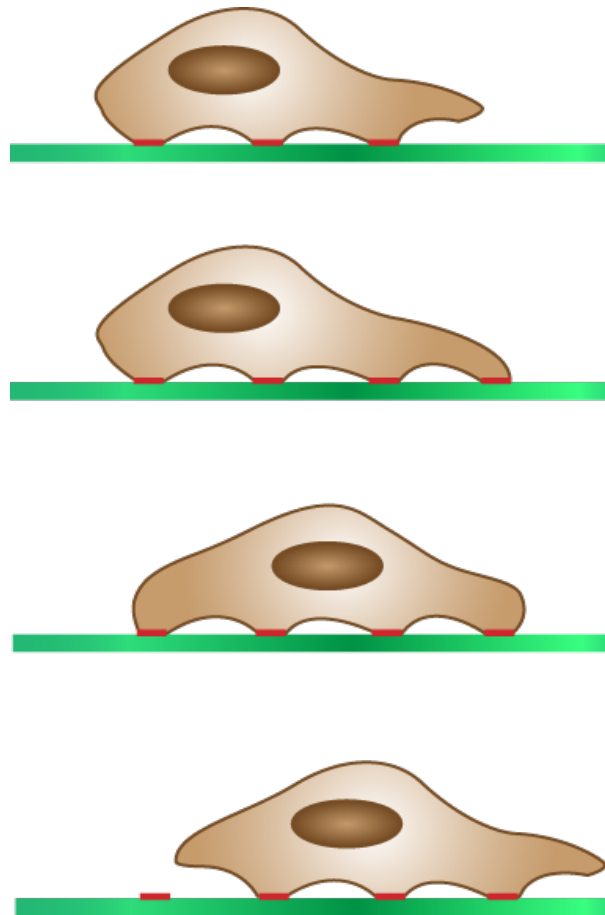


Figure 2. Schematic representation of a cell displacing, where the red spots corresponds to the adhesion points in the surface.

points to exert traction in order to push the membrane in a direction, then the cell detach from the extra cellular matrix to make new focal adhesion points. The extra cellular matrix is the group of tissues that surround the cell, like structural proteins (collagen and elastin) and adhesion proteins (laminine, fibronectine).

2.2. Directed cell migration

In a normal state the cells can migrate to random directions, however when the movement shows a preferred direction it is said that is a directed migration.

There are several forms to induce migration, such as chemotaxis, durotaxis, galva-

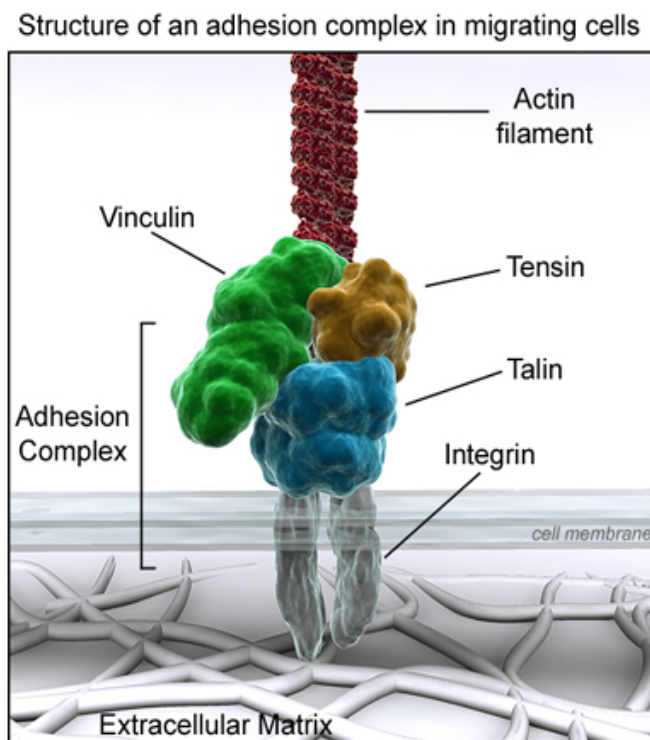


Figure 3. Structure of an adhesion complex in a migrating cells.

notaxis and haptotaxis.

Chemotaxis is the directed migration due to changes in chemical concentration, durotaxis is due to changes in sheer stress of the surfaces where the cell is placed, galvanotaxis is due to changes in electric currents and haptotaxis is due to changes in the properties of the adhesion sites (ChunHong *et al.*, 2012).

2.3. Microfluidics

Microfluidics is the study of the behaviour of fluids constrained to small geometries. This dimensions allow us to have reduced volumes, optimizing the waste of solvents to make experiments. Normally, if one dimension of the channels goes down to few micrometres it is considered to have microfluidic properties.

Microfluidics give us many properties of our interest, one of them is that it provides

laminar flow, this means that if two substances are flowing by two different channels and then the channels get to a joint, the substances will not mix due to the flow and will follow together, if the flow rates are equal, both substances will fill the same volume. Another property is slow diffusion, which means that the only mixing process that will occur in the channel will be given by diffusion.

2.3.1. Laminar flow

It is said that a fluid motion is laminar if the fluid is flowing parallel to the surface and it is not mixing due to perpendicular currents. In fluid mechanics, the characteristics of the flow is determined by the Reynolds number. This number come from the second law of newton for fluids as shown in (Hakho *et al.*, 1991). When this law is applied to fluids it is convenient to consider labelling some set of material points (imagine placing a small amount of dye in the fluid) and following their motion through the system. In addition, we can think about the hydrodynamic pressure as a force acting to either accelerate the fluid elements (i.e. overcome the inertia) or to overcome friction (viscosity) to maintain the motion. Then, it follows that the mechanical response to pressure forces that cause flow depends on the relative magnitude of the inertial response to the viscous response; this ratio is known as the Reynolds number. Therefore in order to obtain laminar flow in a given system it is needed to archive lower Reynold numbers than 2000 (Squires and Quake, 2005).

To have an idea of the order of magnitud, we can aproximate the Reynolds number by direct substitution of the analisis of a sphere of radius l traveling at speed U through a liquid with viscosity μ and density ρ . The Reynolds number can be approached by equation 1 (Hakho *et al.*, 1991).

$$R = \frac{ma}{F_v} = \frac{\rho U l}{\mu}. \quad (1)$$

The Reynold number is a dimensionless parameter since it is a ratio between forces. It is useful to characterize the flow situation for a given system; it is not a simply property of the fluid but rather combines fluid properties (density and viscosity), geometrical properties (length-scale) and the fluid velocity.

To calculate a better approach to the Reynold number a fluid dynamics study is needed. From basic physics we know that every fluid system (liquid or gasses) is linked to the continuity equation that is given by equation 2(Hakho *et al.*, 1991).

$$\frac{\partial \rho}{\partial t} + \nabla(\rho \mathbf{U}) = 0, \quad (2)$$

where the gradient operator is, $\nabla = (\partial/\partial x, \partial/\partial y, \partial/\partial z)$.

Since we are interested in liquids it is better to add the incompressible flow condition to our theoretical description, to find results easier to understand. This means that the pressure variations that accompany the flow create insignificant density changes $d\rho$ i.e. ($d\rho \ll \rho$). Hence, the density of the fluid can be treat as constant.

From this condition and the equation 2 we can see that $\nabla \mathbf{U} = 0$, using rectangular cartesian coordinate system $\mathbf{U} = (U_x, U_y, U_z)$ and the continuity equation is constrained to the allowed velocity variations and is written

$$\frac{\partial U_x}{\partial x} + \frac{\partial U_y}{\partial y} + \frac{\partial U_z}{\partial z} = 0. \quad (3)$$

If we make a momentum analysis in the Navier-Stokes equations (Hakho *et al.*, 1991).

$$\rho \left(\frac{d\mathbf{U}}{dt} + \mathbf{U} \cdot \nabla \mathbf{U} \right) = -\nabla \rho + \mu \nabla^2 \mathbf{U} + \mathbf{F}_b, \quad (4)$$

where \mathbf{F}_b represent the body forces acting on the liquid.

The left hand of the equation 4 refers to the product of masses and acceleration (Newton's second law) and the right hand of the equation 4 refers to forces acting on the fluid.

This equation does not have an analytical solution, but we can make an approximation of it when we have very well known conditions.

If we analyse the flow a little bit away from the inlet and outlet, for relative low flow speeds and perfect uniform channel under incompressible flow, the non linear term ∇U in the equation 4 is zero making it easier to solve and giving rise to steady state solutions. Therefore, for low Reynolds number we have a steady state solution for our systems.

If the solution is a steady state then $U(x,y,z,t) = U(x,y,z)$ simplifying the Navier-Stokes equations to:

$$-\nabla p + \mu \nabla^2 \mathbf{U} + \mathbf{F}_b = 0. \quad (5)$$

The equation 5 only have as parameters the flow speed and the geometrical properties of the microfluidic channels, making it easy to control the conditions to have laminar flow.

2.3.2. Slow diffusion

Diffusion refers to the movement of molecules from a region to another one of lower concentration by random molecular motion.

If laminar flow is guaranteed, then, when two different solutions are injected in the same channel they will not mix due to the flow and will only mix due to diffusion, giving as a result an homogeneous mixture between the fluids.

2.4. Microfluidics for biology

With the aid of a microfluidic system chemical gradients can be done. It had been proven that for a christmas tree arrangement as shown in figure 1, the profile that can be obtained is directly proportional to the number of inlets, being a polynomial of order $N-1$ where N is the number of inlets. The mathematical demonstration can be find in (Dertinger *et al.*, 2001).

It has been proven that a linear profile of epidermal growth factor is enough to stimulate directed migration, therefore a two inlets microfluidic system is enough to study this phenomena (Wang *et al.*, 2013).

Chapter 3

Fabrication of microfluidic devices

The fabrication process of the microfluidic device starts with the fabrication of the master, a mold made of SU-8 2050 MicroChem photoresist to cast the microchannels with PDMS. It consist in 5 main steps.

The first one is the cleaning of the substrate. This step is important in order to have a good adhesion of the photoresist. It is followed by the deposition of the photoresist by spin coating and a baking process. The third step is the exposure, where the sample is set on a photo masker machine with the desire design and then irradiated with UV light. After that, a post exposure bake is required followed by a develop. Finally, it is required to stop the developing process, this is done with a rinse of the sample with isopropanol until all the unexposed photoresist is removed.

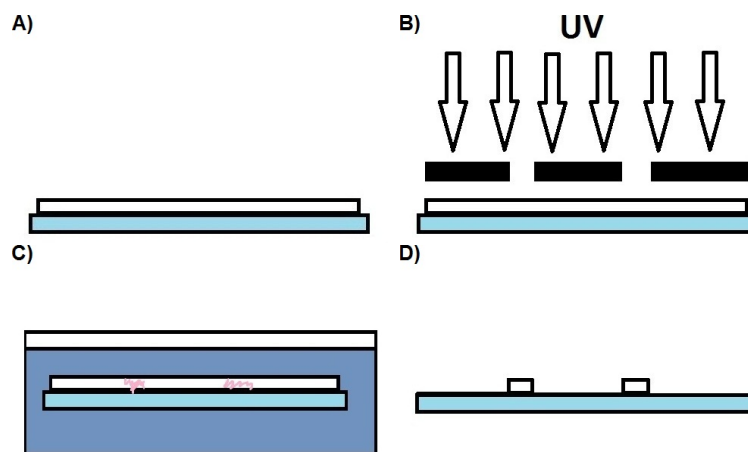


Figure 4. General steps of the photolithography process. A: Photoresist deposit by spin coating. B: Exposure to UV light. C: Development of the device in SU-8 developer. D: Cleaning of the unexposed photoresist with isopropanol.

The general scheme of the process is show in figure 4 and will be described each step in the following sections.

3.1. Soft Lithography

When trying to achieve a good master device that could be used several times, many problems that could arise need to be taken into account. The complexity of the design plays an important role during this process, the parameters or methods could differ highly from design to design.

3.1.1. Cleaning of the substrate

A clean substrate is very important to obtain good adhesion of the photoresist to the substrate, therefore, it is necessary to have a well defined process to do it.

The cleanse of the substrate is performed with the next steps:

- Pre clean the substrate with acetone using a tissue
- Rinse with water
- Dry with an airgun
- Put the sample in a deionized water ultrasonic bath for 5 minutes
- Put the sample in a isopropanol ultrasonic bath for 10 minutes
- Put the sample in a deionized water ultrasonic bath for 5 minutes
- Dry with an airgun

The ultrasonic cleaning process is shown in figure 5



Figure 5. Photography of the ultra sonic bath process to clean the substrate.

3.1.2. Deposition by spin coat

To deposit the photoresist on the substrate we placed the substrate on the spin coater, we dropped a 200ml photoresist then the sample was spin coated in two steps, the first one is to get an initial spread of the photoresist at 500 rpm for 15 seconds and a second one to get the desire thickness at 2000 rpm for 30 seconds. The spin coater used is shown in figure 6.



Figure 6. Photography of the spin coater at the clean room.

3.1.3. Pre-exposure bake

After having the photoresist of approximately 100 micrometres thick layer in the substrate, the sample was taken to a baking process. It was placed in a hot plate at 65 °C for 5 minutes for a soft bake(SB) then at 95 °C for 15 minutes for a hard bake(HB) and finally letting it cooldown for 10 minutes to avoid cracks by stress due to the changes of temperature during the irradiation process.

3.1.4. Exposition

Then the sample was exposed to UV light for 12 seconds getting a radiation dose of 102 mJ/cm². To find out the correct dose for the sample, several tests were done before archiving the correct dose. The photomasker used is shown in figure 7.

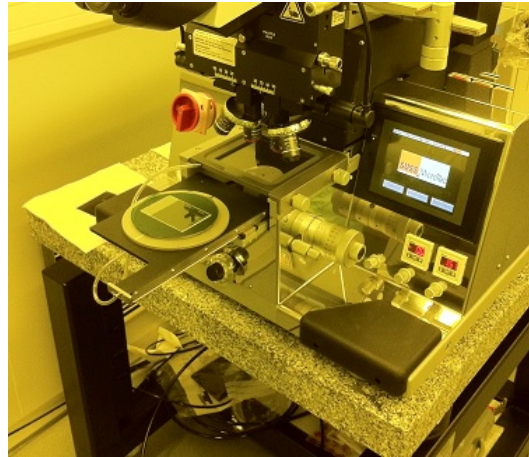


Figure 7. Photo of a device ready to be exposed in the photo masker

3.1.5. Post-exposure bake

A post exposure baking was done with the same temperatures for 4 minutes at 65 °C and 9 minutes at 95 °C as shown in figure 8. Then we wait 10 minutes for cooldown

The standard parameters used for the baking process can be found in table 1



Figure 8. Photography of the hot plates with two devices under the hard bake step.

Table 1. Parameters used in the baking process.

Pre-Exposure SB (min)	Pre-Exposure HB (min)	Cooldown (min)	Post-Exposure SB(min)	Post-Exposure HB (min)	Cooldown (min)
5	15	10	4	9	10

3.1.6. Developing process

After the samples was exposed it is necessary to remove the non exposed photoresist to obtain the desire pattern, to do this the sample need to be developed. We used MicroChem SU-8 developer to perform it.

When trying to use the standard development procedure suggested by the photoresist provider(MicroChem), the main problem that can be found is the inconsistency of the technique in the develop process. MicroChem suggest a technique based on the user skills, a manual develop, where there is no real control of the process, making it

Table 2. Tests done for manual development, showing no real success in being a reliable process.

Develop Time(min)	Photoresist between channels	Overdevelop
5	yes	no
6	yes	no
7	yes	no
8	yes	no
9	yes	no
10	yes	yes
11	yes	yes

unrepeatable. When following the suggested process by MicroChem to produce the gradient generator master, the photoresist was stuck between the closest channels, making it useless.

The table 2 shows the result of the developing tests for the MicroChem suggested technique. It can be seen that we could not achieve any kind of success with it.

It is important to have a well characterized process that can avoid at least, long manual interactions. For this, it was attempted several different processes to optimize the developing process. In the first attempt, the sample was sunk in a falcon tube filled with developer and put to vortex. A great decrease of the developing time was observed, going down from 8-10 minutes (large variation in time based on shaking speed and size of the container) to 3 and a half minutes but the photoresist was not completely removed from the channels before overdeveloping the sample. In table 3 the results using the vortex are shown.

After the vortex, we tried a combine technique with the previous methods (vortex + manual) to develop. After several attempts it seemed inconsistent regarding the develop

Table 3. Tests done for vortex development, shown to be a reliable process but not as accurate as needed.

Develop Time(min)	Photoresist between channels	Overdevelop
1.5	yes	no
2	yes	no
2.5	yes	yes
3	no	yes
3.5	no	yes

time due to manual interactions. We tried a third technique which consist of developing with ultrasonic bath, obtaining very good results and a dramatical reduction of time spent during developing. Going down from the initial 8-10 minutes to 45 seconds as show in table 4. Better results were observed when using the ultrasonic bath in sweep mode.

Even when 45 seconds and 50 seconds presented optimal conditions, we have selected to use 45 seconds in order to avoid overdeveloping due to the time taken in removing the sample.

In order to test the strength of the photoresist we ran three tests. The first one was blowing with an airgun, the second one was making soft contact with the structure and the third one was scratching lightly with a tweezer, where the numbers from one to one hundred its a estimation of the damage made to the structure, by looking at it at the microscope after testing it. Tests results are shown in table 5.

It was found that having an irradiation power of $8.5 \text{ mJ/cm}^2\text{s}$ the correct exposition time to have the strongest adhesion of the photoresist was 12 seconds giving 102 mJ/cm^2 for the radiation dose as seen on table 5. An example of a master device is shown in figure 9.

Table 4. Tests done for ultrasonic development, showing an optimum development time of 45 seconds.

Developing Time	Photoresist between channels	Overdevelop
25	yes	no
30	yes	no
35	some	no
40	few	no
45	no	no
50	no	no
55	no	yes
60	no	yes

3.2. Casting process with Polydimethylsiloxane (PDMS)

Before starting the casting process with PDMS it is necessary to prepare the master to have optimal conditions. Having a hydrophobic surface will prevent the adhesion of the PDMS after baking. Fluorsilane needs to be managed in an chamber filled with argon because fluorosilane reacts with oxygen, therefore is necessary to avoid exposing the floursilane to oxygen. We first introduce a recipient in a chamber filled with argon, after that we put a tissue soak with 100ml of liquid fluorosilane in the recipient and extract it from the argon chamber. We put the recipient in a vacuum chamber with all the master devices to coat and made vacuum for 90 seconds, this ensure that the pressure inside the vacuum chamber gets to the vapour pressure level of the fluorsilane making a change of state from liquid to gas. In order to secure that condition is fulfilled, the master devices was left inside the closed vacuum chamber for 20 hours in order to get them coated with fluorosilane by vapour deposition. When opening the vacuum chamber

Table 5. Tests done for exposition time, showing a 12 seconds exposition time under a UV lamp power of 8.5 mJ/cm²s.

Exposition Time	Airgun	Soft contact	Scratching damage percent
7	yes	yes	-
8	no	yes	-
9	no	no	50
10	no	no	40
11	no	no	40
12	no	no	20
13	no	no	30
14	no	no	50
15	no	no	80
16	no	no	100
17	no	no	100
18	no	no	100
19	no	no	100
20	no	yes	100

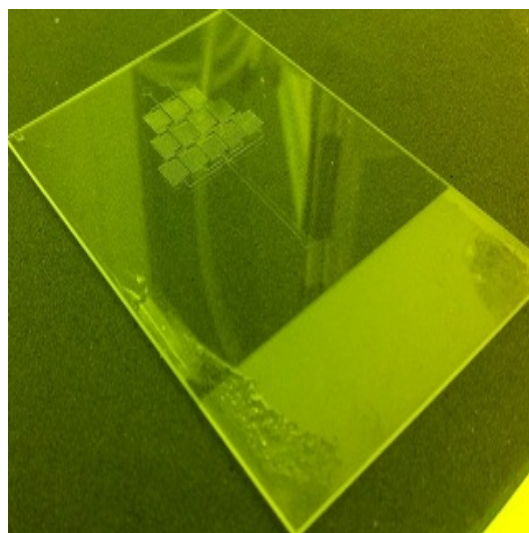


Figure 9. Master device after development. It can be seen some photoresist in the edges in the edges of the substrate.

to extract the devices, it is necessary to do it in a extractor chamber to evacuate the fluorsilane gas. The fluorsilane used was Perfluorodecyltrichlorosilane(FDTS).

To prepare the PDMS that will be used to make our microfluidic device, we mix liquid silicone with the curing agent in a rate ten to one (30g of PDMS + 3g of curing agent). In order to do this we measure the weight in a chemistry balance.

After mixing, a lot of bubbles appeared, so it is necessary to place the PDMS in the vacuum chamber in order to pop up the bubbles. The time needed to remove the bubbles depends on the quantity of PDMS. For a quantity of 33 grams it takes 30 minutes.

The next step is to put the coated master in a container and fill it with the PDMS, we used a glass petri box like container. The last step is baking, it is done in a conventional oven for 2 hours under 75 °C.

When the PDMS is baked, it is recommended to cut it and lift it up it from the master device while it still warm to have an easier detachment. To cut the PDMS a surgical knife was used. It's important to have a very sharp edge to avoid cracking the

PDMS. A cracked PDMS could lead to a bad sticking in the glass substrate due to inhomogeneity on the surface.

After the PDMS is cut to the desire shape it is recommended to unstick all the corners first then help out with the knife to starting lifting the PDMS slowly. When the PDMS is extracted from the master device it can be stored it on dust-free tape for future use.

The PDMS is stored as is ready to be punched in order to make the inlets and outlets for the microfluidic network where needed.

3.2.1. Punching Inlets

The inlets of the microfluidic device needs to be punched before bonding the PDMS in the a glass cover slip to avoid braking it. To make them, we used a piece of a cut syringe needle.

3.3. PDMS bonding by means of Reactive-Ion Etching (RIE)

Reactive-ion etching (RIE) uses chemically reactive plasma to remove material deposited on wafers. The plasma is generated under quasi-vacuum pressure by an electromagnetic field. Ions with very high energy are generated in the form of a plasma to attack the wafer surface and react with it.

The plasma is initiated in the system by applying a strong electromagnetic field. The oscillating electric field ionizes the gas molecules by stripping them of electrons, creating a plasma. This striped electrons are accelerated in the chamber striking the sample at a very high speed. When the electrons drift toward the wafer, they collide with the sample and if the electric field is high enough it can knock off material in the substrate.

Oxygen plasma is very effective in the breaking of most organic bonds of surface contaminants. This helps to break apart high molecular weight contaminants, making them react and due to the vacuum the residue tend to vaporize resulting in a easy extraction of them. At the end of the process the substrate is very cleaned and ionized.

PDMS is hydrophobic, with a low energy and non reactive surface, therefore it is difficult to bond it with other surfaces. By exposing PDMS to oxygen plasma its surface becomes hydrophilic and more reactive. This results in a irreversible bonding when it gets in contact with glass, silicon, or even another PDMS piece that was exposed to the same oxygen plasma. Contact should be made quickly after plasma exposition because the PDMS surface will undergo reconstitution to its hydrophobic and non reactive state within hours. The bonding is accelerated if a post-bake at 75 °C is performed to help remove the humidity between the surfaces.

When the PDMS is exposed to the oxygen plasma the methyl surface groups (Si-CH₃) along the PDMS backbone are transformed into silanol groups (Si-OH) by the reactive oxygen species in the plasma. The glass is also activated by the oxygen plasma producing silanol groups. If both wafers are put in direct contact, the silanol groups can be bonded and converting into siloxane-groups (Si-O-Si) + H₂O as shown in figure 10 and figure 11.

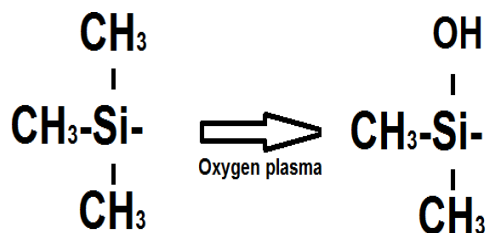


Figure 10. methyl group transformed into silanol group.

In order to bond the PDMS to a glass substrate, we used oxygen plasma.

For the oxygen plasma we found the appropriate parameters for a good bonding,

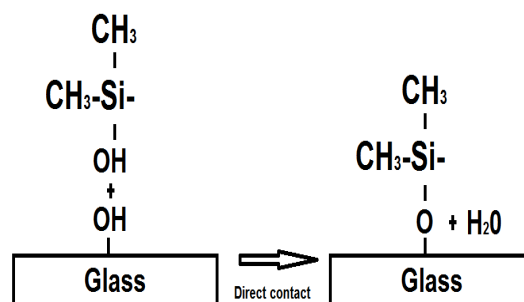


Figure 11. Silanol group transformed into siloxane group.

Table 6. Tests done for RIE process. Optimal parameters are highlighted.

Sample	Power(W)	Time(min)	Bonded
1	50	2.5	no
2	50	3	no
3	20	2.5	not the edges
4	3	3	yes

the runs are showed in the table 6

It is shown that a power of 50W over 3 minutes at 50mTorr was enough to bond the PDMS to the coverglass.

After taking out the bonded sample by oxygen plasma, it is placed in a hot plate at 75 °C for 10 minutes to eliminate humidity in the glass and ensure a safe sticking.

3.4. Tubing and pressure control

To set the proper tubing for the microfluidic device we used Tygon Flexible tubes glued with Loctite silicone as shown in figure 12. To inject the desire fluids, we used a double syringe pump, the PHD ULTRA from Harvard apparatus.

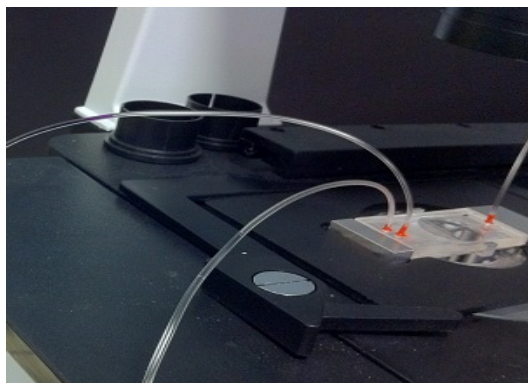


Figure 12. Photography of the microfluidic system tubed.

3.5. Optimizing the process

Since the master device was only lasting 5 uses approximately we decided to optimize the process in order to make more durable masters.

3.5.1. Dilution

The most difficult part of the process was working with SU-8 photoresist due to its high viscosity, making it easy to have a failure. Because of this, we tried a diluted solution with cyclohexanone($C_6H_{10}O$) to reduce its viscosity.

We made a dilution of SU-8 2050 at twenty percent (4-1) using a magnetic stirrer for 2 hours. Then we made thin layers at different rpm to characterize the new photoresist. The height of the layer was measure with Taylor-Hobson Surtronic 3+ perfilometer. The results are shown in figure 13.

Since we are interested in channels with 120-80 microns height, the SU-8 was to diluted to be useful for our device. On the other hand, the management of it improved alot. Its low viscosity made it easy to deposit, therefore, making it useful for a first layer deposition to enhance the adhesion of the photoresist.

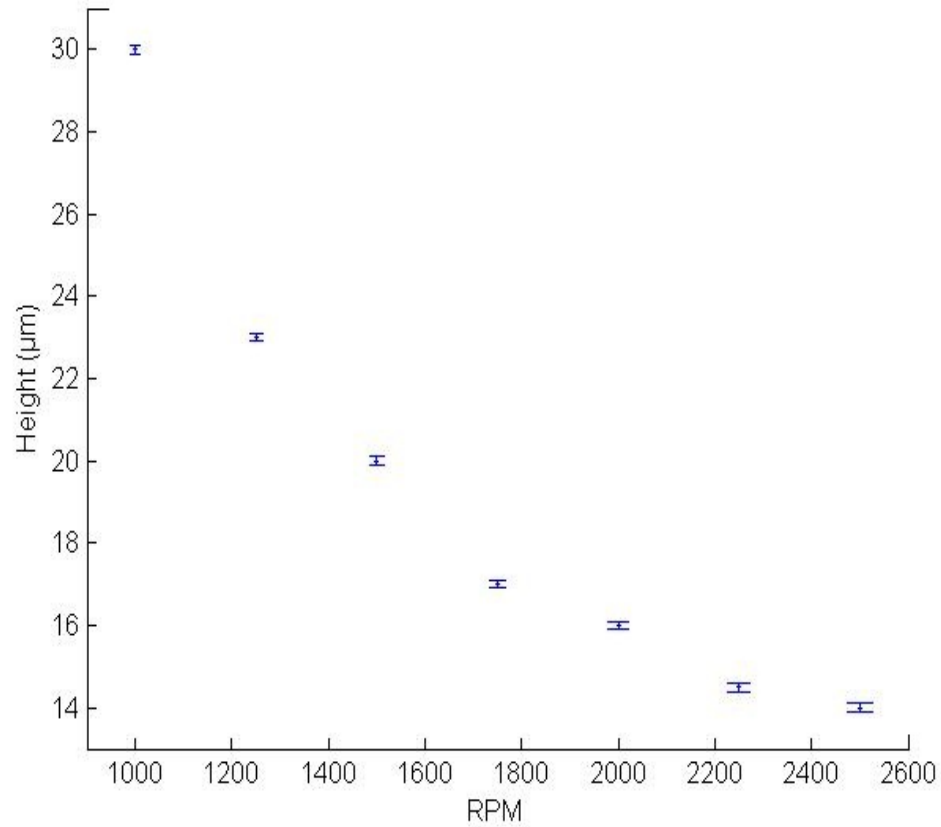


Figure 13. Correspondence between photoresist layer thickness and the rotational speed of the spin coater for a 20 percent diluted SU-8 2050 in cyclohexanone.

3.5.2. Double Layer

The cleaning of the substrate is a key step when working with very small designs. To overcome difficulties and have a better bond, we added first a layer of SU-8 photoresist of 30 micrometres to enforce the bond between the photoresist and the substrate.

Due to the high viscosity of the SU-8 2050 photoresist we used the diluted one at twenty percent for the first layer to ensure a layer with a very homogeneous distribution.

Adding this step improves the lifetime of the master device.

3.5.3. Optimal Parameters

After testing all the parameters we obtained a very good set of parameters for easy manufacturing a robust master device and a well bonded microfluidic device.

Spin coating a first thin layer of 30 micrometres to enhance the bonds between photoresist and the glass. This was made with a SU-8 diluted in volume 1:4 in cyclohexanone (C₆H₁₀O). The spin coating speed used was 1000 rpm for 30 seconds.

A second spin coating of SU-8 to obtain the desire thikness. For a thikness of 80 micrometres it is better to first spin coat at 500 rpm for 15 seconds to spread the resin due to its high viscosity and then spin coat at 2000 rpm for 30 seconds to obtain the desire thickness.

- We used the standard baking times of pre-exposure soft bake (5min), pre-exposure hard bake (15min), post-exposure soft bake (4min), post-exposure hard bake (10min). The temperature used for soft baking was set to 65 °C while the temperature for hard bake was set at 95 °C
- The exposition time was 12 seconds using a dose of 102 mJ/cm²s
- The developing time under ultrasonic(sweep mode) was 45 seconds
- The baking time for PDMS was 2 hours under 75 °C
- A RIE power of 50W over 3 minutes at 50mTorr pressure was used to stick the PDMS to the substrate. After that the sample is placed in a hot plate at 75 °C for 10 minutes

Chapter 4

Experimental methods

Since we are researching in a multidisciplinary area of science, different methods are needed to complete the goal. Different techniques in microscopy, microfluidics and cell culture were used.

In microscopy, we used conventional microscope to observe our devices, fluorescent microscopy to characterize our gradient generators and reflection interference contrast microscopy (RICM) to observe cells. From microfluidics, we made a gradient generator based on slow diffusion and laminar flow. In biology, we made cell culture and tried to develop a technique to cell culture under microfluidic environment.

4.1. Microscopy

Microscopy is the technical field of using microscopes to view samples and objects that cannot be seen with the unaided eye (objects that are not within the resolution range of the normal eye). There are three well-known branches of microscopy: optical, electron, and scanning probe microscopy.

Optical and electron microscopy involve the diffraction, reflection, or refraction of electromagnetic radiation/electron beams interacting with the specimen, and the subsequent collection of this scattered radiation or another signal in order to create an image, while scanning probe microscopy forms images of surfaces using a physical probe that scans the specimen.

4.1.1. Reflection Interference Contrast Microscopy (RICM)

To observe cell migration we need to be able to detect adhesion points very close to the surface. RICM can give information of the distance from the surface to the cell from few nanometres up to 1000nm, it give us quantitative information about the process of adhesion and the evolution of the adhesion points as the cell moves along the surface. RICM also give us information about the shape of the cell. It was first used to observe cell adhesion in the early 1960 by Curtis (Curtis, 1962).

Reflection Interference Contrast Microscopy (RICM) is a microscopy technique that can be used to characterize thin films (Gingel and Todd, 1979) or cells (Hahn and Beck, 1981) in the vicinity of a glass slide illuminated by a monochromatic light source. This technique consist of collecting the light reflected by the surface and the light reflected by the sample and if the distance cell/surface is sufficiently small, on the order of magnitude of the wavelength of the light, successive reflections on the glass slide I_1 and on the cell I_2 will lead to interference. Figure 14 shows a general scheme of the process.

The position and contrast of the interference can be traced back to the distance $h(x)$ between the substrate and the sample, very accurately. Thus, the intensity obtained depends on $h(x)$. The relation between the intensity and the distance $h(x)$ is given by equation 6 (Hakho *et al.*, 1991).

$$I(h(x)) = I_1 + I_2 + \sqrt{I_1 I_2} \cos \left[\frac{4n\pi h(x)}{\lambda} \right], \quad (6)$$

where n is the index of refraction of the medium and λ the wavelength of the light.

Measuring and comparing absolute intensities is a delicate operation. In the context of RICM, if the geometry of the object to be observed is known, this knowledge can often be exploited to devise an alternative to height determination from the intensity. Such a

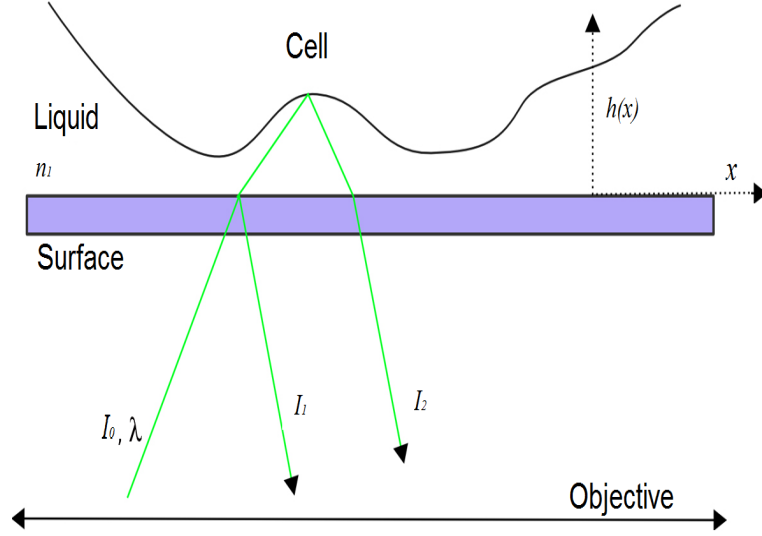


Figure 14. RICM principle: A monochromatic light of intensity I_0 and wave length λ is sent to a cell adjacent to a surface. There formation of interference between the beams reflected by the surface of intensity I_1 , and those reflected by the cell of intensity I_2 . n_1 is the refractive index of the medium. The measurement of the interferogram provides the distance $h(x)$ between the cell and the coverslip.

symmetry-based analysis is often more robust than an analysis based on quantification of the intensity.

In the context of colloidal beads, the geometry of the object is known and is spherical. For the configuration of figure 15 it is expected to give rise to fringes with circular symmetry. A change in the height of the bead changes this fringe pattern in a systematic manner. Using equation 6 and the equation of the sphere with an offset in the vertical axis we can find a equation for the distance from the surface given by the equation 7 (Hakho *et al.*, 1991).

$$h(r_m) = \frac{\lambda(2m-1)}{4n} - R + \sqrt{R^2 - r_m^2}, \quad (7)$$

where R is the radius of the bead, λ the wavelength, r_m the radius of the m maximum fringe from the center and n the index of refraction of the medium.

An image of an a experimental RCIM setup is show in figures 16, 17 and 18. It

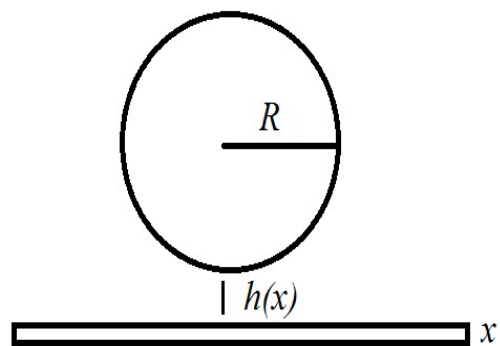


Figure 15. Representation of a spherical bead of radius R separated a distance h from the surface.

consist of an inverted microscope equipped with antireflex objective (only the light coming from the sample is collected in the detector) of 63x magnification, a light source and a CCD camera. The sample is observed under epi-illumination of a monochromatic source, the microscope system is shown in figure 18.

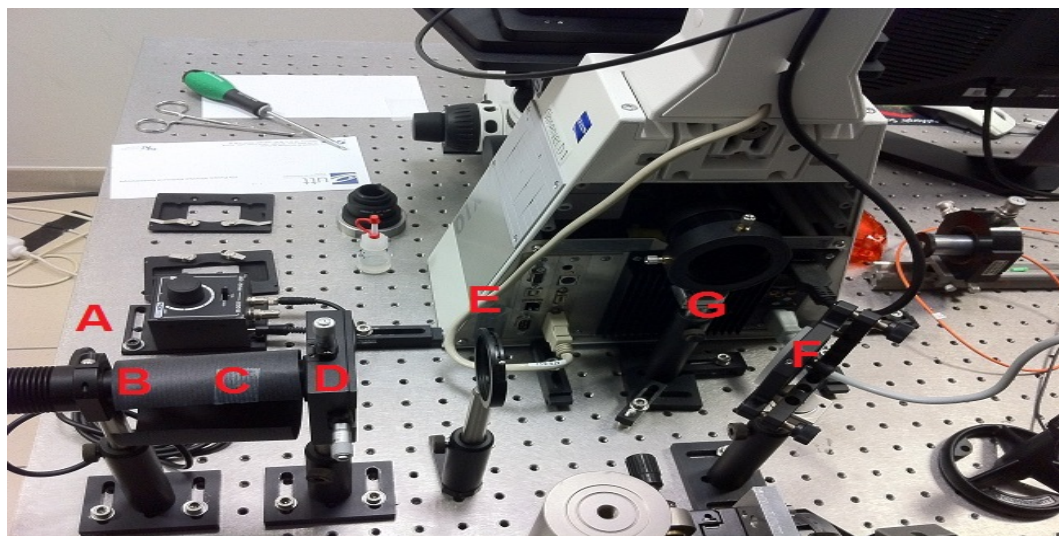


Figure 16. Picture of the system components at LNIO. A is the photodiode, B is the aspherical lens covered in black paper, C is the diffuser covered in black paper, D is a converging lens, E is the diaphragm, F is the mirror and G is a converging lens.

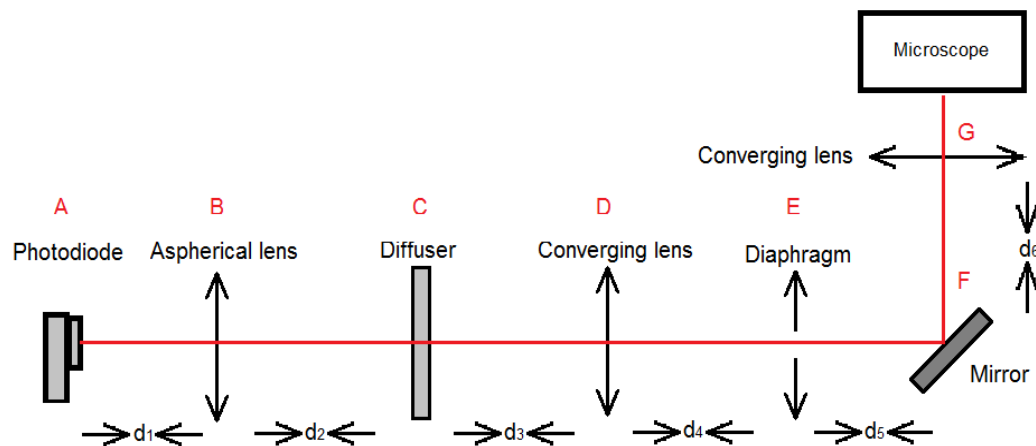


Figure 17. Schematic diagram of the illumination system for the RICM. Letters A to G are relating to figure 16 components.

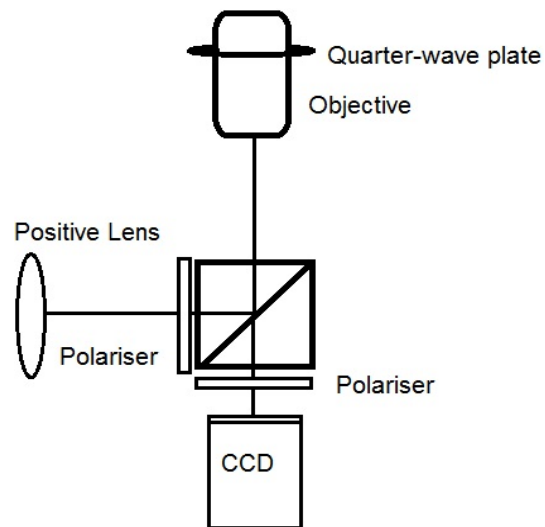


Figure 18. Schematic diagram of the microscope components, showing 2 crossed polarisers, dichroic mirror, CCD camera and a objective with a build in quarter-wave plate.

To build the RICM setup we used the following optic elements:

- ZEISS inverted microscope with a microscope objective of numerical aperture of 0.55 and working distance of 2.6mm
- Photodiode with $\lambda = 658\text{nm}$
- Aspherical lens with a focal length of 6cm.

- Diffuser
- 2 Converging lenses
- Diaphragm
- Mirror

The light from the photodiode is sent through the aspherical lens to collimate it. Then we put a diffuser to avoid the projection of the image of the source in the microscope. After this we set a condenser system using two positive lenses, a diaphragm and a mirror to adapt the system to the space in the table.

The diaphragm needs to be positioned in the focal distance of the first positive lens. The total distance between the lenses (sum of both focal lengths) is determined by the entrance of the microscope.

Since RICM works with interference fringes, the light source should be partially coherent to avoid speckle. For the light source a photodiode and a set of optical components is enough to have an homogeneous illumination at the entrance of the microscope, because of this, manual alignment is necessary.

From figure 16, the distance between photodiode and aspherical lens is $d_1=6\text{cm}$, the distance between aspherical lens and diffuser is $d_2=4\text{cm}$, the distance between diffuser and converging lens is $d_3=12\text{cm}$, the distance between converging lens and diaphragm is $d_4=16\text{cm}$, the distance between diaphragm and mirror is $d_5=8\text{cm}$ and the distance between mirror and converging lens is $d_6=8\text{cm}$.

An inverted microscope is suggested since the samples of interest tend to sediment in the floor of the substrate. A reflector cube inside the microscope needs to be placed in the light path. It should be composed of a polariser, a semi-reflecting mirror and

a cross polariser in order to avoid heavy noise background due to internal reflecting beams.

A special objective is also recommended, an objective that include a built-in quarter-wave plate (QWP) located in front of the lens. With the QWP we ensure that the incident beam and the reflected beams have a crossed polarization, therefore, only the reflected beam will be collected in the CCD camera as shown on figure 18.

As stated previously, most of the time the samples of interest for RICM are sediment in the substrate, commonly a glass coverslip of refractive index 1.52 and surrounded by an aqueous medium (mostly water based mediums of refractive index 1.33 or slightly higher).

The samples used to characterise and test RICM measurements were:

- Glass beads of radius $10\ \mu m$ and refractive index of 1.5
- MDA MB 231 Breast Cancer Cells

4.1.2. Characterization of the RICM

To characterize RICM, experiments were made with spherical beads.

We obtain images of $10\ \mu m$ spherical beads under RICM configuration. The interference pattern is shown in figure 19. The interference pattern look like newtonian rings as expected.

Since we are using particles with a circular geometry, circular integration is optimal to obtain the interferogram. Therefore the localization of the center of the bead is required. We took all linear profiles of the whole matrix (horizontal and vertical profiles) then we selected the ones corresponding to the area of the bead, we found their maximum and the position of the adjacent minimums. Then we choose the linear profile

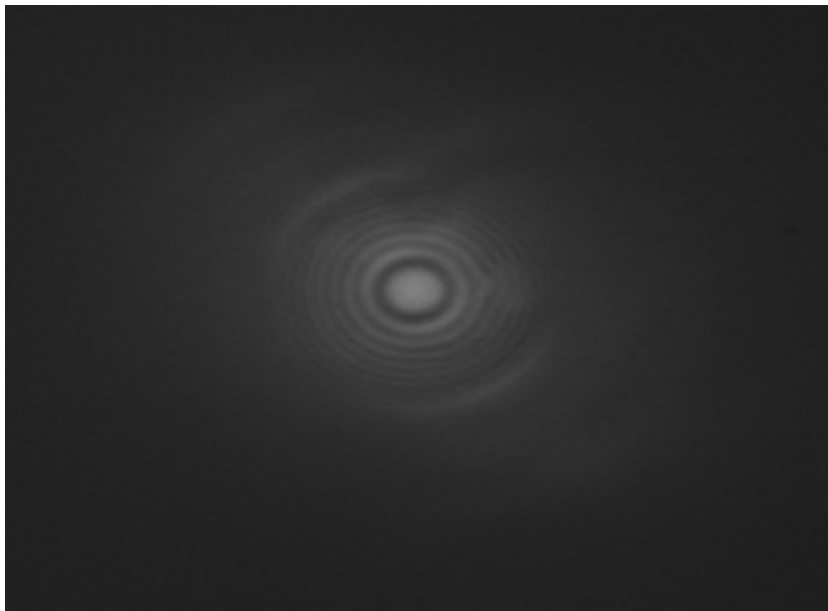


Figure 19. Interference pattern of a spherical bead.

with the maximum separation distance between those minimums to get our coordinates as show in figures 20 and 21.

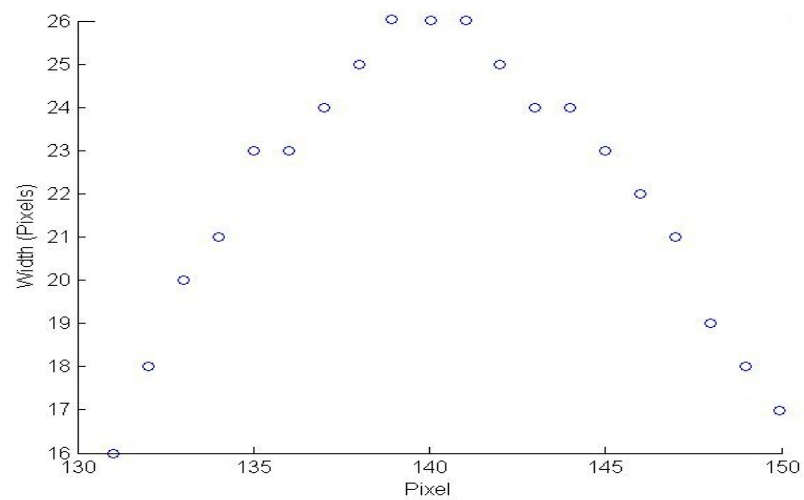


Figure 20. Correspondence between the position and the width in the horizontal axis.

The center for this image is (140,120). The figure 22 shows the position of this pixel. Starting from the center of the bead we made circular integration to obtain the in-

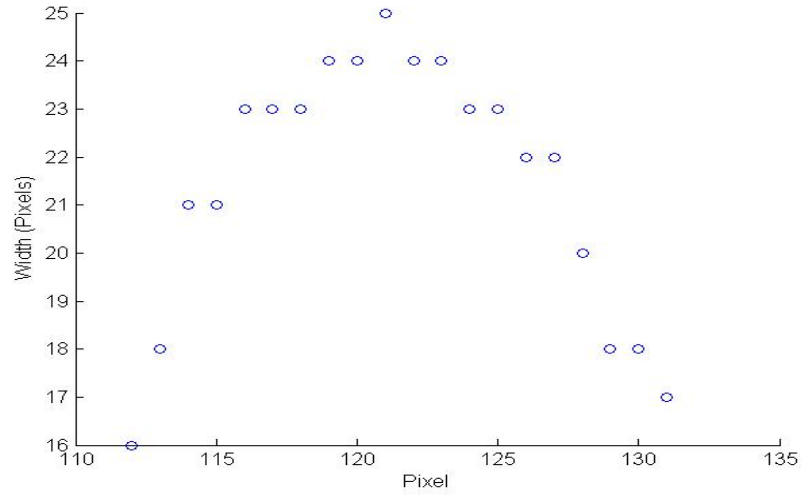


Figure 21. Correspondence between the position and the width in the vertical axis.

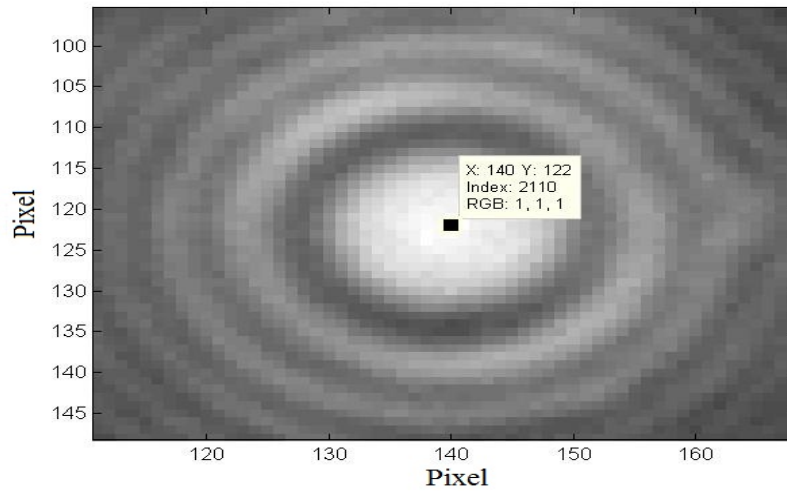


Figure 22. Image of an spherical bead interference pattern and the calculated center pixel.

tensity profile, shown in figure 23. The maximums were found using the matlab function `findpeaks`.

Since the integration was circular, the distance from the center is given by the radius of the circles.

Having the intensity profile, we can find the position of the maximums and by equation 4 we know that every maximum represent a known value of $h(x)$. Therefore

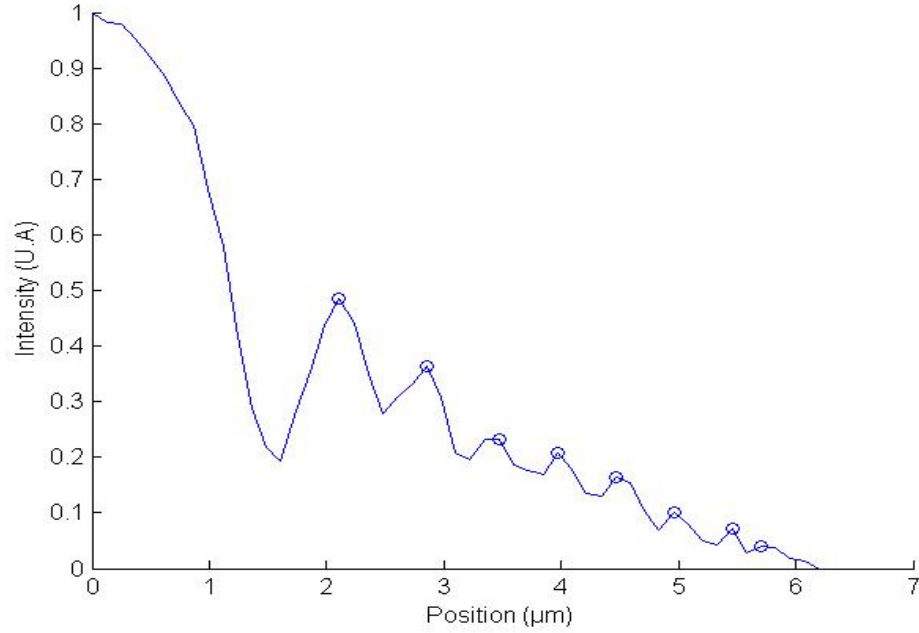


Figure 23. Correspondence between the position and the intensity.

we can plot a graph of $h(x)$ vs distance using equation 7.

Since the object was a sphere, circular profile is expected, therefore, we made a circular fit using Taubin algorithm (Taubin, 1991). The radius value of the fitted circle by the Taubin method was $R=10.018\mu\text{m}$, which shows that using RICM we can retrieve the radius of the sphere very accurately. Knowing the geometry of the object, we can apply the equation 7 to calculate the distance from the surface. The calculated distance of the bead from the surface was $0.389\mu\text{m}$. The results are shown in figure 24

4.1.3. MDA MB 231 cell observation

After testing the RICM with spherical beads, we sedimented MDA MB 231 cells to observe them with RICM and phase contrast microscopy. We used phase contrast microscopy to take a general picture of the cells and RICM to obtain information about the area of contact of the cell.

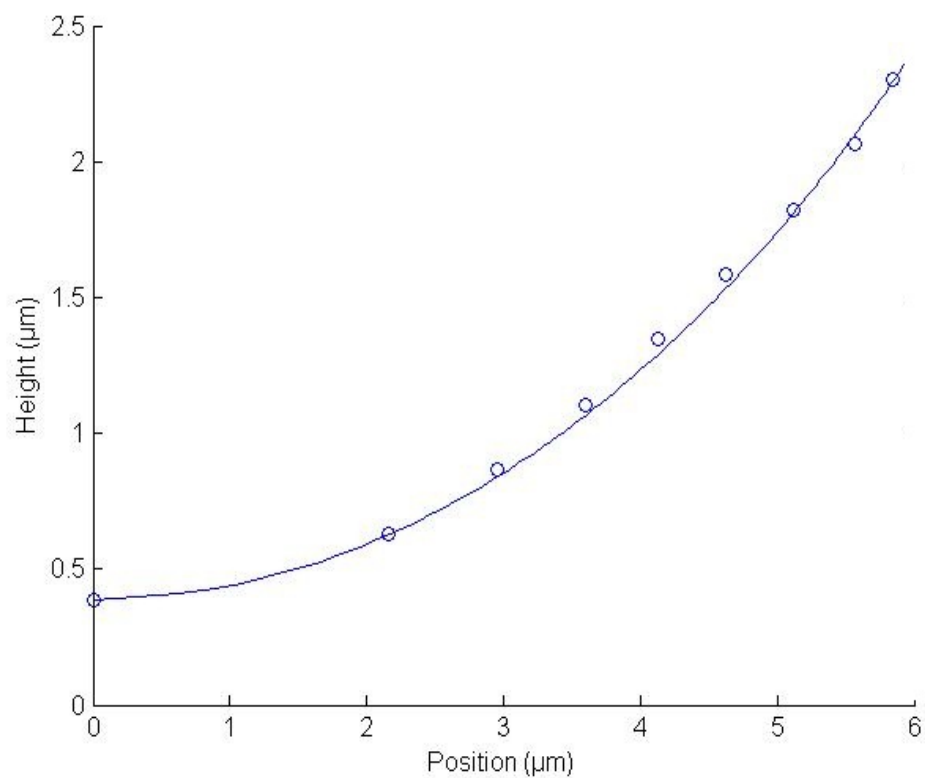


Figure 24. Correspondence between the position of the maximums and the distance from the surface.

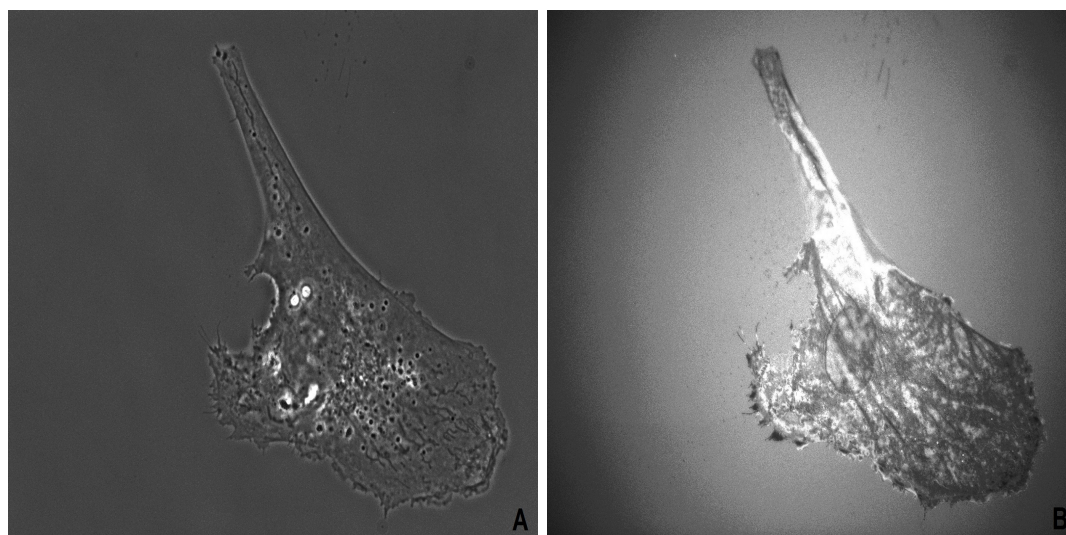


Figure 25. A: Picture of the cell in phase contrast. B: Picture of the cell in RICM.

When we are observing cells under a microscope, it is difficult to say the distance from the substrate to the cell because the cell is composed of different substances. Therefore, the index of refraction of the cell is not constant. In figure 25, we have a cell that had a preferred direction of movement before sticking to the surface. In figure 25b the head of the cell is darker, it means that is very close to the surface, while the tail lighter, meaning that is not close to the surface.

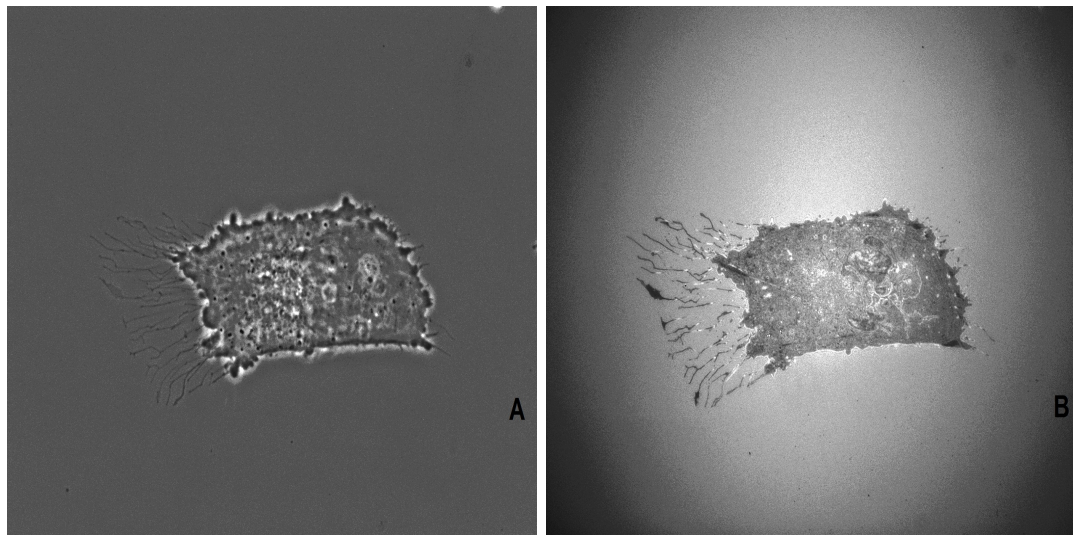


Figure 26. A: Picture of the cell in phase contrast. B: Picture of the cell in RICM.

In figure 26b, shows an image of a cell under RICM, the edge of the lamellipodium is completely dark while the rest of it is white, it can be because the cell is moving to the right using the lamellipodium as traction.

In order to use RICM for quantitative experiments a more complex system is needed. Labelling the cells with fluorescent quantum dots would ensure low area of contact, therefore, interference patterns.

4.2. Gradient generator

A gradient generator is a device that can ensure a spatial concentration profile of a solution given two starting solutions with different concentrations by controlled mixing. It was first designed by (Stephan *et al.*, 2000). It consist of a microfluidic network that mixes the initial solutions. The arrangement if known as a christmas tree microfluidic network as shown in figure 1.

The gradient generator microfluidic device was made in PDMS with a channel height of $80\ \mu\text{m}$ and a channel width of $100\ \mu\text{m}$ ensuring the fulfilling of the requirements for microfluidic conditions (laminar flow and slow diffusion) by the equation 1, giving a maximum Reynolds number of 0.01 for a fluid velocity of 0.1 ml/min.

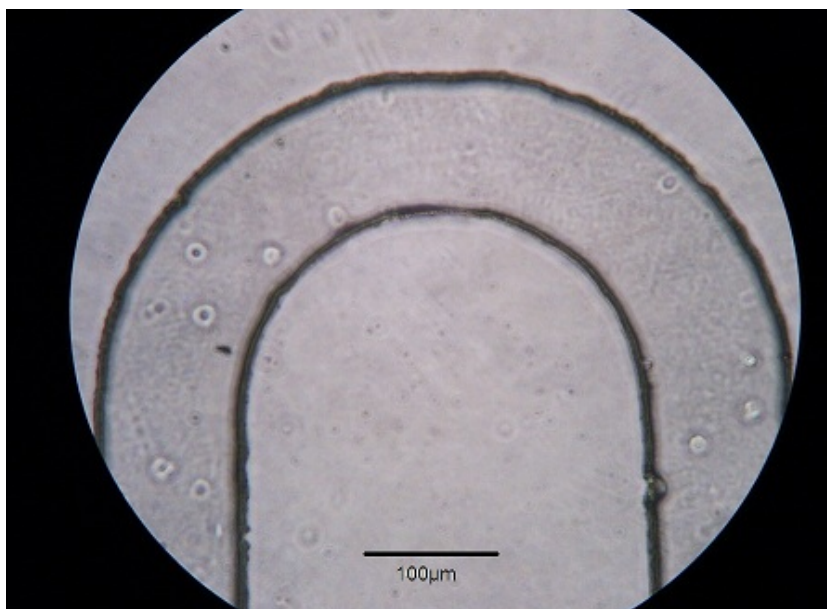


Figure 27. Optical microscopy image showing a microchannel with a U shape of the gradient generator device.

Our gradient generator is formed of mixing channels with different geometries, like straight lines and curves. Figure 27 shows the U turn of our microfluidic device while the figure 28 shows the branching of all mixing channels into the outlet channel.



Figure 28. Optical microscopy image showing a microchannel of a five channel joint of the gradient generator device.

4.2.1. Mathematical description

Using the fundamental properties of microfluidics we can induce chemotaxis for the study of cell migration through the concentration of epidermal growth factor (EGF) (Price *et al.*, 1991).

A simple model that describes the behaviour in the microchannels of the volume splitting ratios under laminar flow is using a description analogous to the analysis of an electric circuit. In the microfluidic scheme, the fluid flow represents the current while the viscosity and the length of travel play the role of the resistance. So the flow will go towards the trajectory of minimum resistance.

An approach to generate the gradients is using a microfluidic network in a Christmas tree configuration geometry, as shown in figure 29.

A simple way to describe a branching point is shown in figure 30, where we just take care about 1 inlet and 2 directions of flow. From figure 30 we have the equation

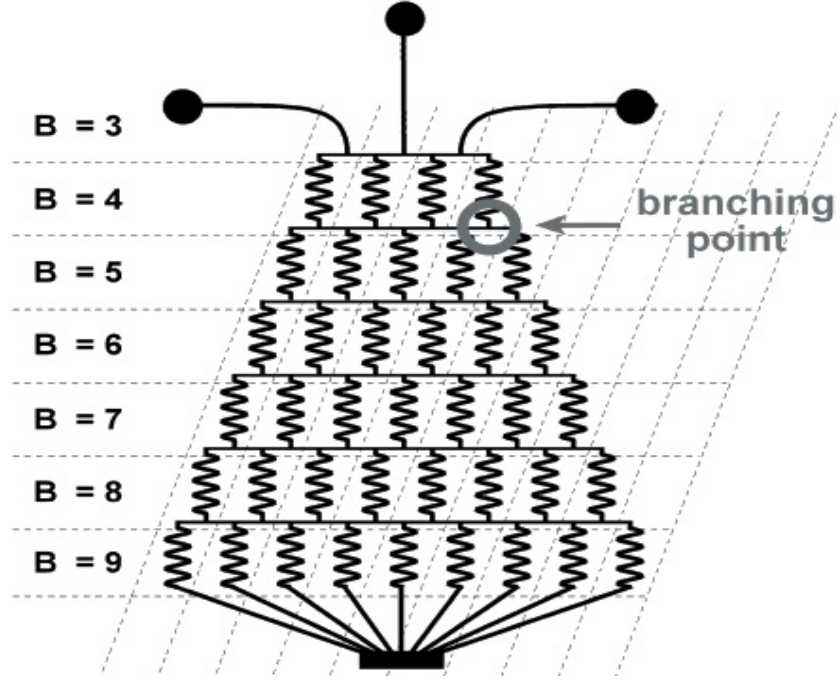


Figure 29. Christmas tree microfluidic network geometry.

for the joint.

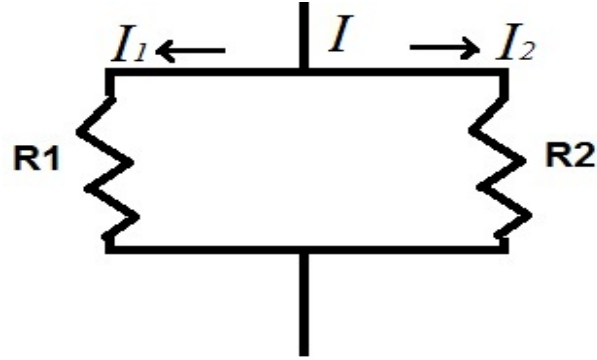


Figure 30. Equivalent electric circuit model of a single branch.

$$I = I_1 + I_2, \quad (8)$$

where I is the inlet current and I_1 and I_2 are the outlet currents.

By analogy to the ohms law we have that the flow that is needed to satisfy the

following equation is given by (Hakho *et al.*, 1991).

$$I = \frac{V}{R}, \quad (9)$$

where V is the pressure difference and R is the resistance of the channel.

In general $I_n = V/R_n$, where I_n and R_n are the inlet of the n side and the resistance of the n side.

Since the continuity equation (Hakho *et al.*, 1991) needs to be satisfy, the difference in pressure for both ways need to be constant, from the equation 9 we can get equation 10.

$$I_1 = \frac{R_2}{R_1} I_2 \quad (10)$$

If we substitute this in the node equation 8 we obtain an expression in terms of the inlet current.

$$I_1 = \frac{R_2}{R_1 + R_2} I, \quad (11)$$

or in general

$$I_n = \frac{R_m}{R_n + R_m} I. \quad (12)$$

For a symmetrical system we have that $R_1 = R_2 = R$. We can see in the equation 8 that $I_1 = I_2$, but for a general system like the one shown in figure 30, $R_1 \neq R_2$. R_1 and R_2 will be given by the sum of the resistance in each side for each branch of the microfluidic network.

A simple model to obtain a general expression for the splitting of the flow can be obtained using the convention in the figure 31, where every level is marked, with B the

number of inlets in the current horizontal level and S the number of additional resistances to the left from the branching point.

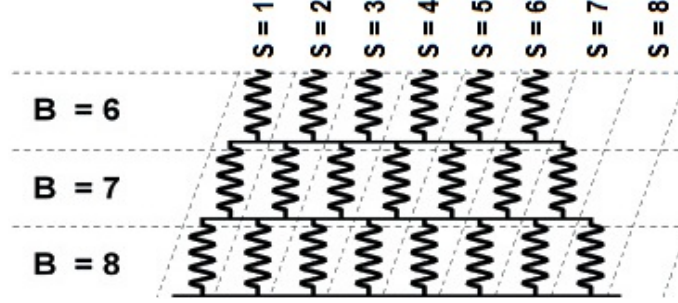


Figure 31. Schematic representation for the nomenclature we used for the mathematical description of the network. If $B=6$ and $S=2$, for this branching point $R_1 = 2R$ and $R_2 = 5R$.

Under this conventions the equations for the currents can be written in the following way (Stephan *et al.*, 2001).

$$I_1 = \frac{B - S + 1}{B + 1} I, \quad (13)$$

$$I_2 = \frac{S}{B + 1} I. \quad (14)$$

Using this convention it is easy to follow the current in every branch in order to know the distribution of the flow. Therefore we can know what percentage of each substance from each inlet goes to each channel.

For a two inlet system like the one shown in figure 29 the total flow in each level B is given by equation 15.

$$I_{tot_B} = \frac{B}{B + 1} I \quad (15)$$

The concentration in the channels on the edges of the system is filled with pure solution coming from the inlets (inlet one for the left sided channels and inlet two for

the right sided channels). The flow for an arbitrary channel (B,S) is given by the two flows of the adjacent branching points, the ratios are given by equations 13 and 14.

$$I_{BS} = I_{B(S-1)_2} + I_{BS1}, \quad (16)$$

where S needs to be $\neq 1, B$.

The concentration is given by equation 17.

$$C_{BS} = \frac{C_{(B-1)(S-1)}I_{B(S-1)_2} + C_{(B-1)S}I_{BS1}}{I_{tot_b}} \quad (17)$$

Using equations 13, 14 and 15 in equation 17 we can find a recursive equation for the concentration.

$$C_{BS} = \frac{(S-1)C_{(B-1)(S-1)} + (B-S+1)C_{(B-1)S}}{B}, \quad (18)$$

where $C_{B1} = C_{11}$ and $C_{BB} = C_{12}$. Being C_{11} and C_{12} the concentration at the inlets.

4.2.2. The mixing chamber

To ensure diffusion for Reynolds numbers lower than 1, long mixing channels are suggested (Stephan *et al.*, 2001), this let us change the inlets velocity without losing the laminar flow property nor the slow diffusion.

The mixing chamber consist of a serpentine channel. Its total length is given by 10 straight segments of 3400 μm and 13 turns of middle radius 150 μm , giving a total length of 40.13 millimetres. The outlet channel width is 1 millimetre and have a length of 14.2 millimetres

4.2.3. The step profile

As a first gradient generator we designed a linear concentration profile generator with two inlets and five outlets. The design is shown in figure 1.

We mounted the microfluidic device in a microscope and then we injected with a syringe pump water in one inlet and Potassium permanganate(KMnO_4) as a coloured substance in the other one and took some pictures at the outlet channel. In order to make a step profile, is required to have high flow velocities to avoid diffusion in the outlet channel. The velocity required to be able to see a step profile was 0.4 ml/minute.

We measure the line intensity profile in two places of the outlet channel, the first one located at 200 μm from the joint of all the channels shown in figure 32A and the second one at 2000 μm from the joint shown in figure 32B.

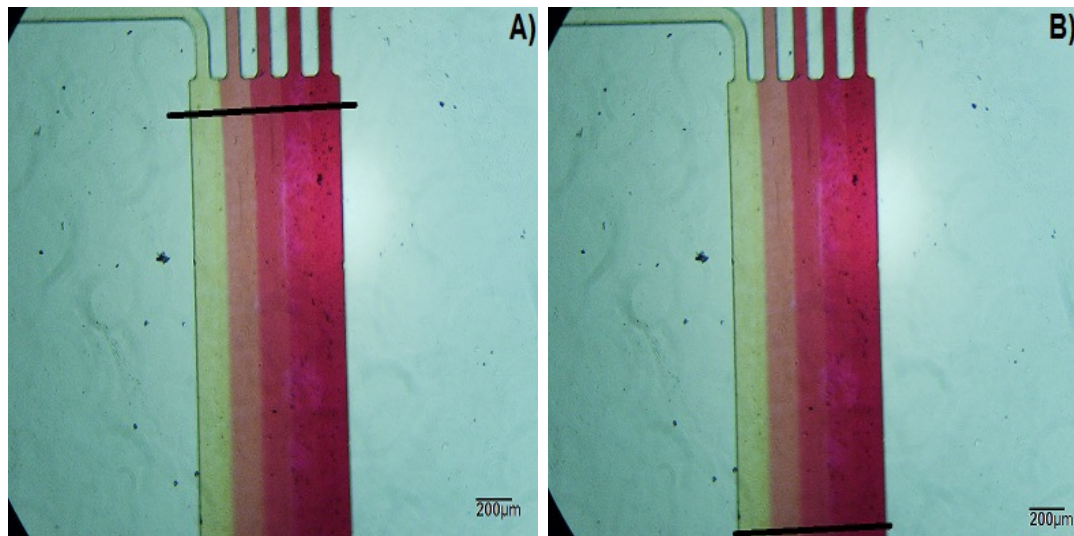


Figure 32. Image of the outlet channel showing the gradient line profile for two different positions along the outlet channel under a flow rate of 0.4 ml/minute. a: 200 μm from the joint. b: 2000 μm from the joint.

At 200 μm from the joint we obtain a step profile for the concentration as shown in figure 33, this is expected since the mixing by diffusion is still occurring in the entrance of the channel. It can be seen in figure 34 that even if the velocity was high, the diffusion

was still going on and tending to get a linear profile when it gets far from the joints. The distance between this two profiles is $1800\ \mu m$, it is less than the half of the length of the mixing chamber, length that ensure diffusion.

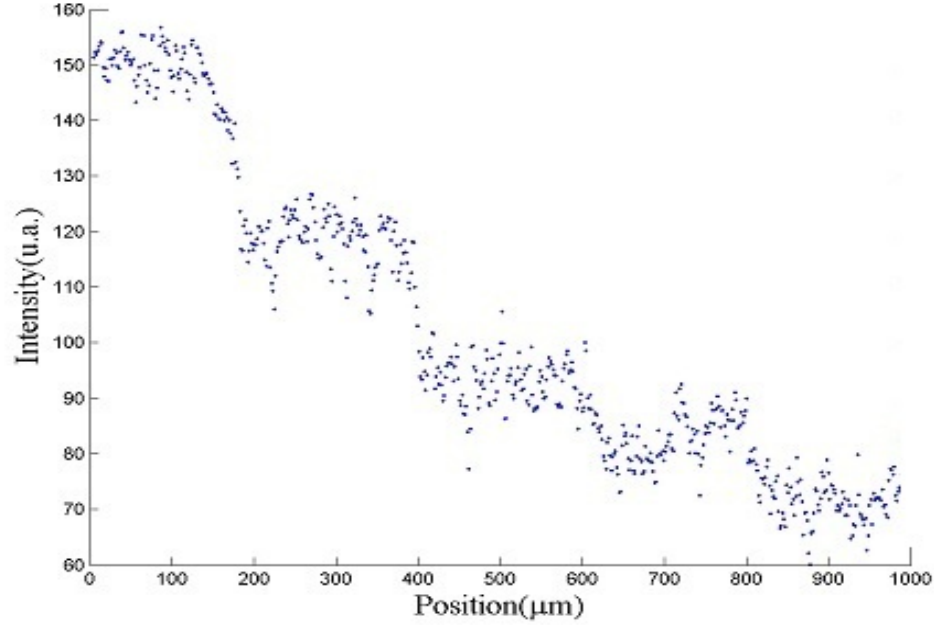


Figure 33. Correspondence between intensity and position at $200\ \mu m$ from the joint for the dye solution experiment.

Then we repeated the experiment with Alexa488 fluorescent probes that absorbs at $\lambda = 495$ and emit at $\lambda = 520$ and using the same gradient generator microfluidic device, multiple images were required because the microscope vision area for fluorescence was limited to the size of the laser spot as shown in figure 35. In this case we also obtain a step profile as shown in figure 36

After looking at the step profile, we lowered the velocity to $0.01\ \text{ml/minute}$ to observe if the behaviour was linear as expected

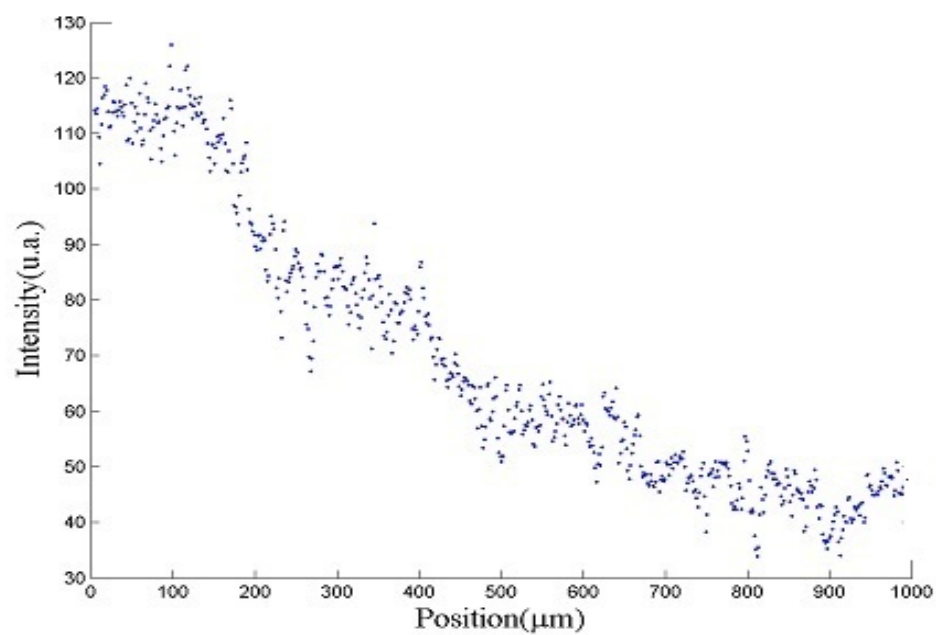


Figure 34. Correspondence between intensity and position at 2000 μm from the joint for the solution experiment.

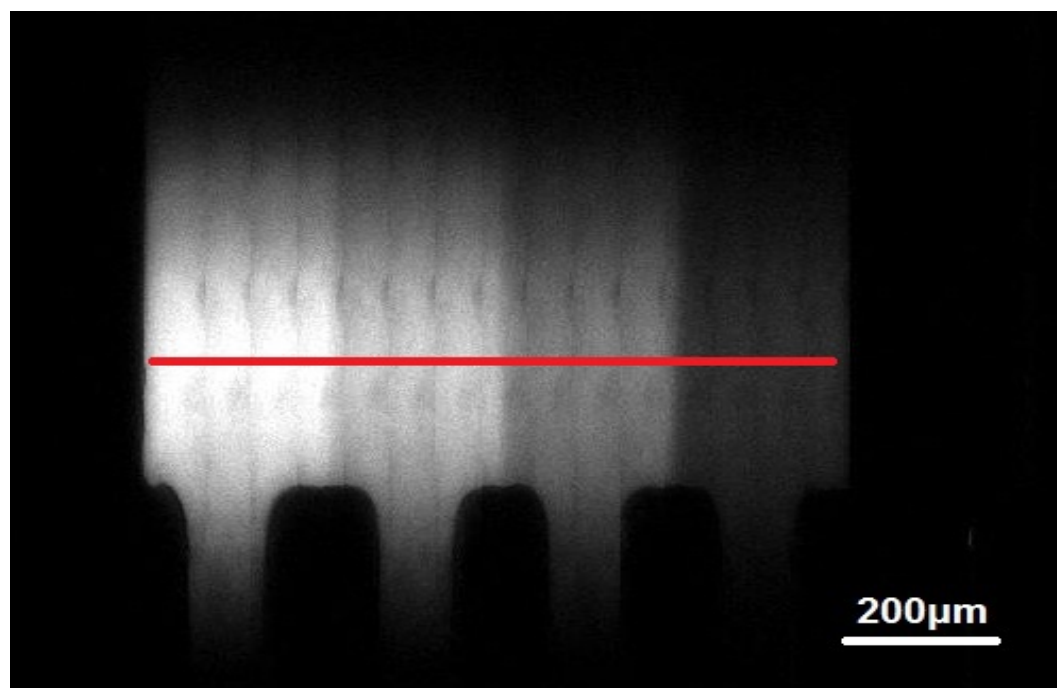


Figure 35. Gradient line profile at 5000 μm from the joint at the outlet channel under a flow rate of 0.4 ml/minute.

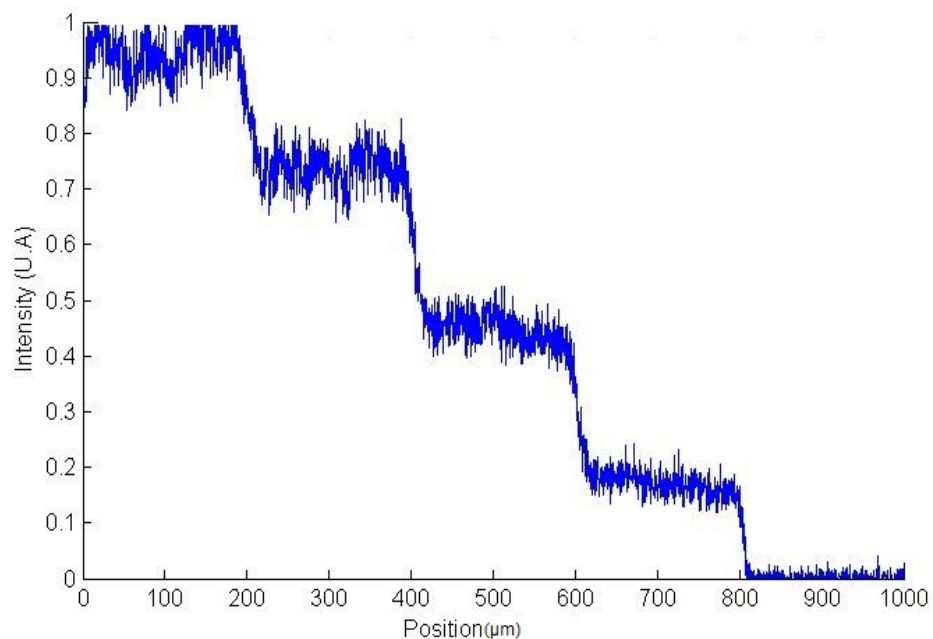


Figure 36. Correspondence between intensity and position at 5000 μm from the joint for the fluorescent particles solution experiment.

4.2.4. The linear profile

To ensure mixing by diffusion we lowered the inlets flow rate to 0.01ml/minute. This velocity is low enough to have diffusion within the length of the outlet channel. We measured an intensity profile of the outlet at a distance of 5 millimetres from the joints. The image line profile its display as the black line in the figure 37 and the profile is shown in figure 38

We obtained a linear profile as shown in figure 38, showing that our gradient generator is working and we are able to produce the desire profile.

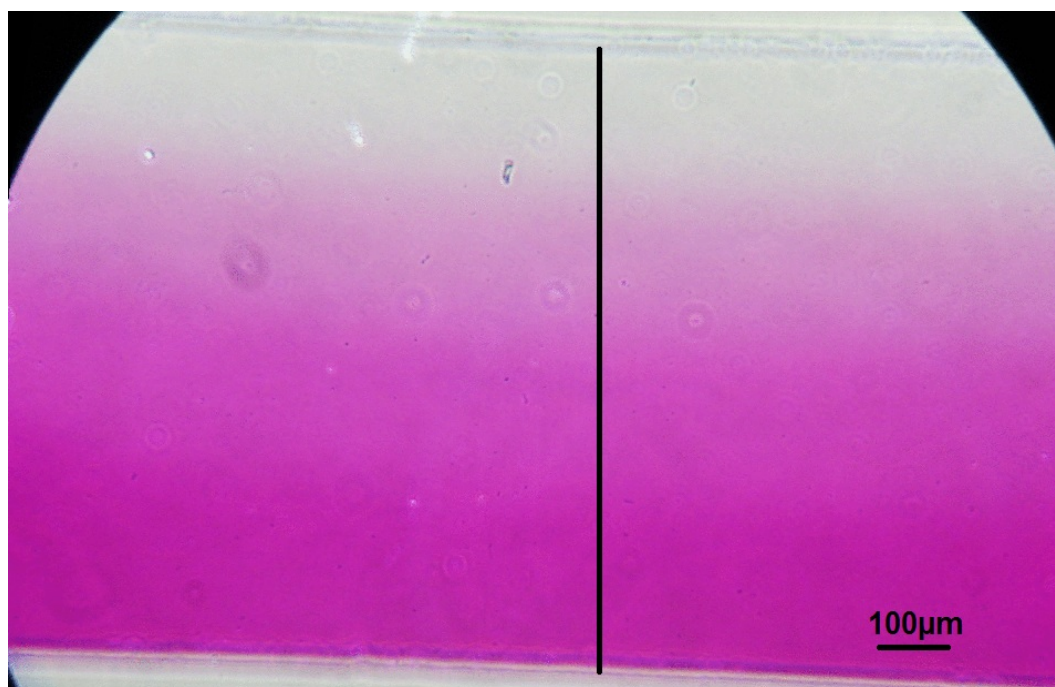


Figure 37. Gradient line profile at 5000 μm from the joint at the outlet channel under a flow rate of 0.01 ml/minute.

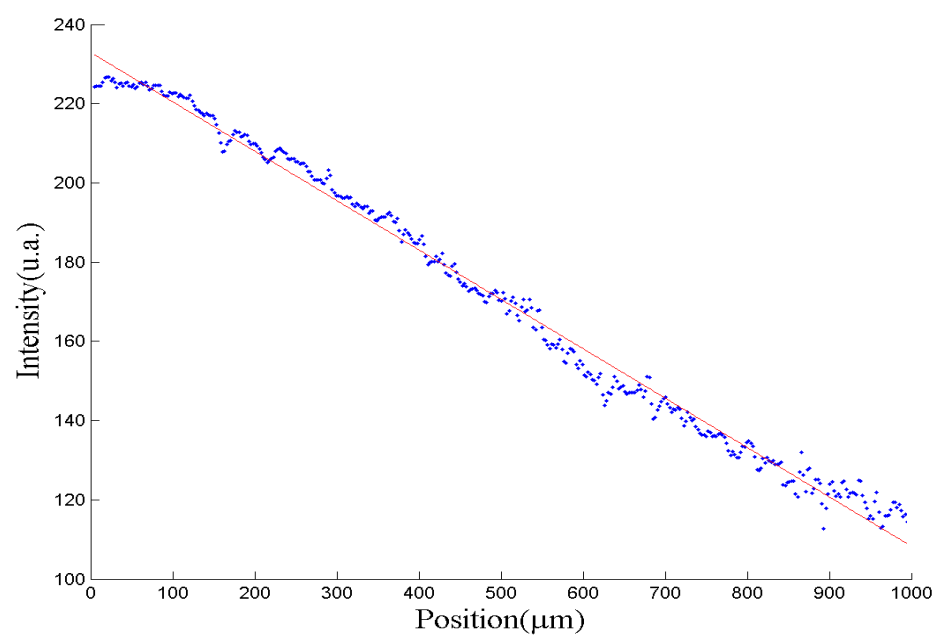


Figure 38. Correspondence between intensity and position at 5000 μm from the joint for the dye solution experiment.

Chapter 5

Cell fixing in microfluidics

In this chapter, we will describe the procedure that we followed for cell fixing in microfluidic device, in this case in a gradient generator. The cells that were inserted to fix were MDA MB 231, breast cancer cells. In order to constantly test our cell fixing technique it is necessary to have a supply of fresh and healthy cells. We will also describe the protocol for cell subculture.

5.1. Maintaining cultured cells

In this section we will describe the procedure for subculturing of cells in culture. Subculturing is a procedure where we remove the growth medium and transfer the cells from a previous culture into a fresh growth medium. In this way we maintain a fresh supply of cells.

The equipment and materials needed for subculture are an incubator at 37 °C with 5% CO_2 atmosphere, cell culture hood and reagents.

The process of cell subculture is pretty standard and consists in the following steps:

1.- Sterilization with alcohol the cell culture hood and all the reagents containers this include:

- Phosphate buffered saline (PBS). It is used to wash the cells in the culture flask.
- Dulbecco's modified eagle's medium (DMEM) + Glutamax. It is the cell culture medium.
- Trypsin. It is a protein for easier cell detachment from the culture flask.

- Culture Flasks.

- 2.- Remove and discard the spent culture medium from the culture flask.
- 3.- Wash cells with 5ml of PBS.
- 4.- Discard the PBS from the culture flask.
- 5.- Add 500 μ l of trypsin
- 6.- Incubate the cell culture flask at 37 °C with 5 % CO_2 atmosphere.
- 7.- Remove the culture flask from the incubator
- 8.- Add 5ml of culture medium in the culture flask and 5ml of culture medium in a new culture flask.
- 9.- Transfer the desire volume to the new culture flask.
- 10.- Label the new culture flask with the following data:
 - Name of the cells
 - Date
 - Initial Volume
 - User name
- 11.- Incubate the culture flasks at 37 °C with 5 % CO_2 atmosphere.

5.2. Cell fixing in a microfluidic device

Cell fixing in microfluidic device is not a well characterized process. In order to try to do cell culture, we followed the next process.

- Flow the medium in the microfluidic device (This is to have the channels already wet)

- Inject cells
- Put the device in the incubator for 1 hour

First we tried to inject the cells directly (before tubing) into the microfluidic device and then we placed the device in the incubator, after 1 hour we observed that the cells were fixed. Then we did the same but adding the tubing, after 2-3 hours the cells started to detach and die. The first thing to considerate was contamination due to the silicone but after seeing this many times even with the most of the cares we discarded this option.

Another factor that could play an important role for cell fixing is the pressure. Since the cells are sensible to pressure and can get stressed by changes of pressure, therefore, as a second option we tried first making the tubing, then, a cleaning of the device for possible silicone leakage, afterwards we filled the tubes and the device with medium and at last we injected the cells. Using this method we intermediately found a problem, we had changes of pressure due to gravitational potential, making the cells flow slowly through the channel until they left the device.

Then as a third attempt, we plugged the tubes of the inlets but did not plugged the tube in the outlet, then we directly injected the cells into the microfluidic device and placed it in the incubator for 1 hour, after this step, the cells were fixed. Then we plugged a metallic tube (a piece of a cut syringe needle) directly in the outlet and on it we plugged a piece of plastic tube, with this, we managed to have a closed system. Figure 39 shows some MDA MB 231 cells inside a microfluidic system.

Since the volume in the microfluidic device are small we have evaporation due to temperature (37°C) which the cells requires to stay alive, it is needed to keep a constant flow of fresh culture medium inside the microfluidic device. When trying to do this we

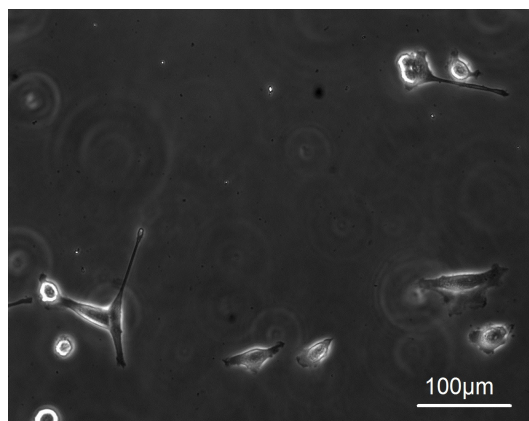


Figure 39. Living MDA MB 231 cells attached in the substrate in a microfluidic device.

got some bubbles going inside the microfluidic channels and since the flow was really slow, the cells died due to lack of culture medium in this period. We tried to overcome this problem by changing how we introduce the culture medium, first connecting the syringes right after adding the cells and second trying doing it at the end, on both cases without success in solving the air bubbles problem.

When trying to work with cells in a microfluidic environment there are many problems to overcome, the main problems we found was pressure problems and in the way to inject the medium to avoid bubbles. We suggest implementing luerstocks to manage the pressure and bubbles problems.

Chapter 6

Conclusion and perspectives

During this research project the necessary basic techniques were studied to fabricate a microfluidic device in order to build an experimental system for measuring the adhesion and movement of cells during the migration process. The process used to produce the microfluidic master device was photolithography using ultrasonic cleaning, deposition by spincoating and ultrasonic development. It was found that one of the main factors affecting the durability of the master device was the developing process. When the developing process is performed it is needed to consider the shape and proximity of the structures because if they are close enough, some photoresist could get stuck between them. Ultrasonic development shows to be a good way to develop the sample. Coating the master device with fluorsilane before using it improved the lifetime of it, making easier to remove the PDMS from the master.

We have presented that RICM as a technique with good accuracy to measure distance from the surface without labelling or staining the sample. Its drawback is the complexity of the image interpretation for complex images especially for quantitative analyses. This issue arises from the fact that RICM measure optical paths rather than absolute distance. Possible future developments could be made with a combination of RICM with other surface microscopy techniques, for example total internal reflection microscopy (TIRF). Another way is to perform a high theoretical and experimental analysis using spectral variation to determinate length independently of material optical properties.

Finally RICM has demonstrated to be compatible with microfluidics due to the

nature of the surfaces. Microfluidic devices are made on glass coverslips, the glass coverslips have a flat surface, therefore are optimal for an RICM setup.

We also presented our ways to do cell culture in a microfluidic environment without having success on keeping the cells alive. More experimental work is needed to be done in order to have a stable environment to keep the cells alive, being the control of the pressure one of the main goals. We propose to lock the inlets with luerstocks to avoid changes of pressure that could stress the cells and additionally avoid the introduction of air bubbles.

We developed an analytic technique to calculate the split ratios of substances with different components, therefore, is possible to calculate the parameters to produce multiple gradients of different components at the same time.

Bibliographic references

- Barr, V., Bunnell, S. (2009). Interference reflectance microscopy. *Curr Protoc Cell Biol*, **12**: 4–25.
- ChunHong, Z., GuiE, C., YuHong, P., YanYi, H. (2012). Microfluidics: An integrated microfluidic device for long-term culture of isolated single mammalian cells. *Science China Chem*, **55**: 502-507.
- Curtis, A. (1962). Cell contact and adhesion. *Rev Camb Philos Soc*, **37**: 82-129.
- Dertinger, S., Chiu, D., Li Jeon, N., Whitesides, G., Choi, I., Stroock, A. (2000). Generation of solution and surface gradients using microfluidic Systems. *Langmuir*, **16**: 8311–8316.
- Dertinger, S., Chiu, D., Li Jeon, N., Whitesides, G.(2001). Generation of gradients having complex shapes using microfluidic networks. *Analytical Chemistry*, **73**: 1240–1246.
- Eddings, M., Johnson, M., Gale B. (2008). Determining the optimal PDMS to PDMS bonding technique for microfluidic devices. *J. Micromech. Microeng.*, **18**: 961–1317.
- Gingel, D., Todd, I. (1979). A quantitative theory for image interpretation and its application to cell-substratum separation measurement. *Biophysical Society*, **26**: 507–526.
- Hahn, B., Beck, K. (1981). Evaluation of reflection interference contrast microscope images of living cells. *Microsc Acta*, **84**: 78–153.
- Hakho, L., Donhee, H., Westervelt, R. (1991). *CMOS Biotechnology*. Springer, New York.
- Haubert, K., Drier, T., Beebe D. (2006). PDMS bonding by means of a portable, low-cost corona system. *Lab Chip.*, **6**: 1548-1549.
- Limozin, L., Sengupta K. (2009). Microfluidics: Quantitative reflection interference contrast microscopy (RICM) in soft matter and cell adhesion. *ChemPhysChem*, **10**: 2752–2768.
- Moraes, C., Wyss, K., Brisson, E., Keith, B., Sun, Y., Simmons, C. (2010). An undergraduate lab (on-a-Chip): Probing single cell mechanics on a microfluidic platform. *Cellular and Molecular Bioengineering*, **3**: 319–330.

- Price, J., Tiganis, T., Agarwal, A., Djakiew, D., Thompson, E. (1999). Epidermal growth factor promotes MDA-MB-231 breast cancer cell migration through a phosphatidylinositol 3-Kinase and phospholipase C-dependent mechanism. *Cancer Res*, **59**: 5475–5478.
- Rupprecht, P., Gole, L., Rieu, J-P., Vezy, C., Ferrigno, R. (2012). A tapered channel microfluidic device for comprehensive cell adhesion analysis, using measurements of detachment kinetics and shear stressdependent motion. *Biomicrofluidics*, **6**: 1058-1932.
- Sengupta, K., Aranda-Espionza, H., Smith, L., Janmey, P., Hammer, D. (2006). Neutrophil spreading: From touchdown to first steps. *BioPhys. J.*, **91**: 4638–4648.
- Squires, T., Quake, S. (2005). Microfluidics: Fluid physics at the nanoliter scale. *Reviews of Modern Physics*, **77**: 977–1026.
- Stephan, K., Pittet, P., Renaud, L., Kleimann, P., Morin, P., Ouaini, N., Ferrigno R.(2007). Microfluidics: Fast prototyping using a dry film photoresist: microfabrication of soft-lithography masters for microfluidic structures. *Journal of micromechanics and microengineering*, **17**: 64–69.
- Taubin, G. (1991). Estimation of planar curves, surfaces and nonplanar space curves defined by implicit equations, with applications to edge and range image segmentation. *IEEE Trans. Pattern Analysis Machine Intelligence*, **13**: 1115–1138.
- Vezy, Cyrille (2004). *Dynamique de billes d'agarose et de vésicules géantes en adhésion sous un écoulement de cisaillement*. Doctoral thesis, L'Université de Technologie de Troyes.
- Wang, S., Saadi, W., Lin, F., Nguyen, C., Li Jeon, N. (2004). Differential effects of EGF gradient profiles on MDA-MB-231 breast cancer cell chemotaxis. *Experimental Cell Research*, **300**: 180–189.
- Winckler, P., Jaffiol, R., Plain, J., Royer P., (2010). Nonradiative excitation fluorescence: probing volumes down to the attoliter range. *J. Phys. Chem*, **1**: 2451–2454
- Whitesides, GM., Ostuni, E., Takayama, S., Jiang X., (2001). Soft lithography in biology and biochemistry. *J. Annu. Rev. Biomed*, **1**: 335–373
- Zidovska, A., Sackmann, E. (2011). On the mechanical stability of filopodia. *Biophys. J*, **100**: 1–10